# Apoptosis restores cellular density by eliminating a physiologically or genetically induced excess of enterocytes in the Drosophila midgut

Rihab Loudhaief, Alexandra Brun-Barale, Olivia Benguettat, Marie-Paule Nawrot-Esposito, David Pauron, Marcel Amichot, Armel Gallet

© 2017. Published by The Company of Biologists Ltd | Development (2017) 144, 808-819 doi:10.1242/dev.142539

STEM CELLS AND REGENERATION

RESEARCH ARTICLE

# Apoptosis restores cellular density by eliminating a physiologically or genetically induced excess of enterocytes in the *Drosophila* midgut

**Rihab Loudhaief, Alexandra Brun-Barale, Olivia Benguettat, Marie-Paule Nawrot-Esposito, David Pauron, Marcel Amichot and Armel Gallet***

## ABSTRACT

Using pathogens or high levels of opportunistic bacteria to damage the gut, studies in *Drosophila* have identified many signaling pathways involved in gut regeneration. Dying cells emit signaling molecules that accelerate intestinal stem cell proliferation and progenitor differentiation to replace the dying cells quickly. This process has been named 'regenerative cell death'. Here, mimicking environmental conditions, we show that the ingestion of low levels of opportunistic bacteria was sufficient to launch an accelerated cellular renewal program despite the brief passage of bacteria in the gut and the absence of cell death and this is is due to the moderate induction of the JNK pathway that stimulates stem cell proliferation. Consequently, the addition of new differentiated cells to the gut epithelium, without preceding cell loss, leads to enterocyte overcrowding. Finally, we show that a couple of days later, the correct density of enterocytes is promptly restored by means of a wave of apoptosis involving Hippo signaling and preferential removal of old enterocytes.

**KEY WORDS: Opportunistic bacteria, Apoptosis, Cellular homeostasis, *Drosophila* intestine, JNK signaling, Hippo signaling**

## INTRODUCTION

In the animal kingdom, the digestive tract (DT) is a vital organ required for nutrient absorption that also constitutes the first barrier against pathogens ingested along with food. In both vertebrates and invertebrates, well-conserved mechanisms of defense have been elaborated to maintain DT epithelial integrity and prevent aggressors from the lumen (the external environment) penetrating into the internal milieu. Among these mechanisms of defense, the DT triggers a cell replenishment program to replace damaged cells rapidly upon injury (Sun and Irvine, 2014).

Many studies have been performed in *Drosophila* to gain insight into the mechanisms underlying intestine regeneration upon pathogenic intoxication or injury (Sun and Irvine, 2014). Deciphering these mechanisms has highlighted the importance of many conserved signaling pathways already known to be required for the maintenance of gut homeostasis under normal conditions. The *Drosophila* posterior midgut epithelium shares some similarity with the vertebrate intestine and consists of four cell types. The basally located intestinal stem cells (ISCs) serve to regenerate each gut cell type. Upon division, ISCs can either give rise to ISCs and/or enteroblasts (EBs). EBs can then differentiate either into absorptive enterocytes (ECs) or secretory enteroendocrine cells (Pasco et al., 2015).

Two Gram-negative bacteria have been primarily used to study gut regeneration upon ingestion: the opportunistic *Erwinia carotovora carotovora* (*Ecc*) and the entomopathogenic *Pseudomonas entomophila* (*Pe*). Large amounts of *Ecc* or smaller amounts of *Pe* lead to EC death (Buchon et al., 2009a, 2010; Chatterjee and Ip, 2009). Indeed, less than 4 h post-ingestion, ECs produce reactive oxygen species (ROS) to fight the ingested bacteria. In the same time window, owing to the cellular damage and death caused by the production of ROS as well as by the ingested bacteria, JNK and Hippo (Hpo)/Yorkie (Yki) stress signaling pathways are activated in ECs. Activation of these pathways results in the nuclear translocation and activation of the transcription factors AP1 (downstream of JNK pathway) and Yorkie (Yki), which induce the expression of cytokine- and growth factor-encoding genes. During the next 24-48 h, those secreted factors act non-autonomously on ISCs, increasing their rate of proliferation to generate more EBs, which then differentiate into new ECs to replace the damaged or dead ones (Apidianakis et al., 2009; Buchon et al., 2009a, 2010; Cronin et al., 2009; Jiang et al., 2009; Kim and Lee, 2014; Kux and Pitsouli, 2014; Lee et al., 2013; Myant et al., 2013; Osman et al., 2012; Ren et al., 2010; Shaw et al., 2010; Zhou et al., 2013). The dedicated process of cell replenishment is termed 'regenerative cell death' and involves damaged and/or dying cells releasing a variety of growth factors and cytokines involved in tissue repair and/or regeneration (Sun and Irvine, 2014; Vriz et al., 2014). Increasing the speed of gut replenishment upon injury helps to maintain the barrier function of the gut epithelium, avoiding the penetration of bacteria into the internal milieu. Failure to replenish the gut lining properly generates holes in the epithelium, facilitating pathogen invasion of the body, ultimately leading to sepsis-induced death (Bonfini et al., 2016).

The studies summarized above were performed using either a large amount of opportunistic bacteria or pathogenic bacteria. However, under normal conditions, the DT is constantly in contact with smaller amounts of bacteria swallowed along with food. Here, using the *Drosophila* adult midgut, we investigated the effect of dietary exposure to low amounts of opportunistic bacteria on gut cellular homeostasis. Surprisingly, ingestion of low amounts of Gram-positive or Gram-negative bacteria, despite their rapid elimination, triggers a cell renewal program, although not inducing intestinal cell death. Consequently, within a couple of days, the newly added differentiated ECs cause an excess of cells, although polarity and integrity of the epithelium are maintained. During this period, the digestive capacities of the gut are significantly diminished. Interestingly, we showed that gut

Université Côte d'Azur, INRA, CNRS, ISA, 06900 Sophia Antipolis, France.

*Author for correspondence (gallet@unice.fr)

**Received 22 July 2016; Accepted 10 January 2017**

Development (2017) 144, 808-819 doi:10.1242/dev.142539

homeostasis is restored 2-3 days after bacteria clearance thanks to a wave of apoptosis preferentially removing old ECs. A similar wave of apoptosis is also involved in elimination of a genetically induced excess of ECs. Finally, we demonstrate that the Hpo signaling pathway is necessary to trigger the wave of apoptosis removing the supernumerary cells.

## RESULTS

### Low levels of opportunistic bacteria induce a mild early stress response in the *Drosophila* posterior midgut

To assess the impacts on the intestinal epithelium of ingesting a small amount of opportunistic bacteria along with food, we chose the Gram-positive *Bacillus thuringiensis var. kurstaki* (*Btk*) because this bacterium is used worldwide as a bioinsecticide in agriculture and therefore could be present at low concentration in food. Moreover, *Btk* is also known as a potent opportunistic bacterium for many organisms (Raymond et al., 2010), and is responsible for, among others, nosocomial diseases and food-poisoning associated diarrheas (Celandroni et al., 2014).

To define what we called 'low doses' of ingested bacteria, we took into account the amount of *Btk* found on vegetables after one aerial spreading i.e. $1\times10^5$ colony forming units (CFU)/g (Frederiksen et al., 2006; Stephan et al., 2014) and the application doses recommended by the manufacturers of *Btk* bioinsecticides, i.e. $5\times10^5$ to $2.5\times10^6$ CFU/cm² depending on the type of crop to treat. Therefore, we exposed adult flies to bacteria by contaminating the culture medium with $1\times10^6$ CFU/5 cm²/fly (referred as $10^6$ CFU in the following text). Flies were then left on the contaminated medium until dissection. *Btk* was completely eliminated from the midgut less than 4 h post-ingestion (PI) (Fig. 1A). The maximal number of bacteria we detected in the midgut was ∼100 CFU, present 1 h PI. We noticed that *Btk* was rapidly cleared from the surface of the culture medium (data not shown) highlighting the fact that flies were not submitted to chronic intoxication. Conversely, when flies were fed with higher levels of *Btk* (e.g. $1\times10^8$ CFU/5 cm²/fly, referred as $10^8$ CFU in the following text) the bacteria persisted for a longer time in the gut (Fig. 1A). Finally, when flies were fed with low doses ($1\times10^6$ CFU) of the commensal Gram-positive bacterium *Lactobacillus plantarum* (*L. plantarum*), the bacteria were still detected in the gut 3 days PI at a dose of $10^4$ CFU/gut (Fig. 1A) (Storelli et al., 2011). Of note, we easily differentiated the food-provided *L. plantarum* from the indigenous *L. plantarum* present in the commensal flora of our *Drosophila* strains as we assessed the amount of indigenous *L. plantarum/brevis* at $1.5\times10^2$ CFU/gut (i.e. 100 times less).

Because small amounts of *Btk* were rapidly eliminated from the intestine, we wondered whether its transient presence could nevertheless trigger a stress reaction in the posterior midgut. Thus, we followed the activation of both JNK and Hpo/Yki signaling pathways by monitoring the expression of their target genes using either *lacZ* reporter genes or RT-qPCR. We found that at 4 h PI the expression of the JNK signaling reporter gene *puc-lacZ* was indeed induced in ECs (Fig. S1A,B). We confirmed the induction of *puc* by RT-qPCR (Fig. 1B). Nevertheless, JNK signaling activation was no longer maintained 24 h PI (Fig. S1G). We did not observe any Hpo/Yki target gene induction [*Diap1* and *expanded* (*ex*)] (Fig. 1B). We next wondered whether ingestion of low levels of the Gram-negative model bacterium *Ecc* could also trigger a brief and moderate stress response by the gut. As expected, ingestion of low amounts of *Ecc* ($10^6$ CFU) induced a similar brief and moderate gut response

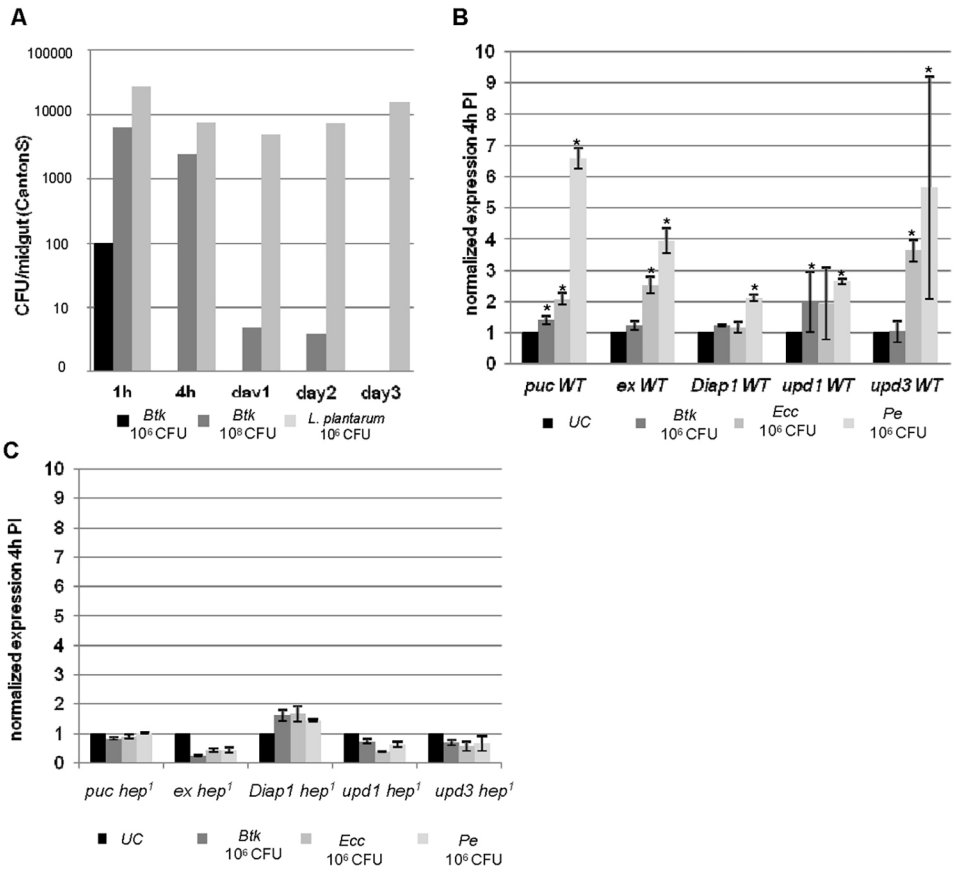


**Fig. 1. A small amount of opportunistic bacteria induces a mild early stress response in the *Drosophila* posterior midgut.** (A) Counting of bacteria in guts (*n*=30) from 1 h to 3 days PI. The initial dose provided with the food to flies was $10^6$ CFU or $10^8$ CFU of *Btk* and $10^6$ CFU of *L. plantarum* per fly/5 cm². (B,C) RT-qPCR on whole midguts 4 h PI. Normalized expression of *puc*, *ex*, *Diap1*, *upd1* and *upd3* are shown (*n*=30). Wild-type (WT) flies (B) and homozygous *hep¹* females (C) were fed with sucrose (unchallenged, UC), *Btk* $10^6$ CFU, *Ecc*$10^6$ CFU or *Pe* $10^6$ CFU.

Development (2017) 144, 808-819 doi:10.1242/dev.142539

although we also noticed an induction of the Hpo/Yki target gene *ex* (Fig. 1B; Fig. S1D,I). As control, we used the commensal *L. plantarum* also at $10^6$ CFU/5 cm²/fly and this did not trigger any stress signaling in the adult gut (Fig. S1K-M).

To fine-tune the read-out of our study, we included two other genes encoding cytokines, *upd1* and *upd3*, which are known to be induced by both JNK and/or Yki signaling in ECs following ingestion of *Pe* or large amounts of *Ecc* and to be responsible for ISC proliferation upon damage (Buchon et al., 2009a,b; Bunker et al., 2015; Jiang et al., 2009; Karpowicz et al., 2010; Osman et al., 2012; Patel et al., 2015; Ren et al., 2010; Shaw et al., 2010; Staley and Irvine, 2010). We found that small amounts of *Btk* activated *upd1*, but not *upd3*, whereas small amounts of *Ecc* activated *upd1* (although not significant in our statistical test) and *upd3* (Fig. 1B). We further compared these results with the stress induced by ingestion of small amounts of the entomopathogenic *Pe* (Fig. 1B) or large amounts of *Btk* or *Ecc* ($10^8$ CFU) (Fig. S1N). As expected, all the target genes were activated. Moreover, the amplitude of *upd1* and *upd3* induction was greatly increased (Fig. S1N). We noticed that the Gram-positive *Btk* preferentially induced *upd1*, whereas the Gram-negative *Ecc* induced *upd3* and *Pe* induced both (Fig. 1B; Fig. S1N). We also observed that when flies were fed with large amounts of *Btk* or *Ecc*, the tissue stress was maintained for a longer time, as highlighted by the prolonged expression of *puc-lacZ* 24 h PI (Fig. S1H,J). Therefore, our data demonstrated that the ingestion of small amounts of opportunistic Gram-negative or Gram-positive bacteria triggers a mild and brief stress response by the posterior midgut.

Because JNK signaling has been shown to be the first stress signaling pathway activated upon huge damage (in less than 30 min) (Buchon et al., 2009a,b; Jiang et al., 2009), we wondered whether JNK signaling was also responsible for the primary response of the gut to a moderate stress. Therefore, we assessed the expression of *puc*, *upd1*, *upd3*, *ex* and *Diap1* 4 h PI in female flies that were homozygous mutant for the loss-of-function allele $hep^1$ [*hemipterous* (*hep*) encodes for the upstream JNK-activating kinase also known as JNKK] fed with either low amounts of *Btk*, *Ecc* or *Pe*. Interestingly, none of these target genes was expressed (Fig. 1C) even with *Pe*. Therefore, the stress response of the gut to the ingestion of small amounts of opportunistic or pathogenic bacteria appears to depend primarily on JNK signaling activation.

### Mild stress induces ISC proliferation and an accumulation of enterocytes

Although the ingestion of small amounts of *Btk* or *Ecc* only moderately induced a stress response by the gut, we wondered whether this was sufficient to trigger ISC proliferation. We first monitored the mitotic indices of ISCs using a phospho-Histone 3 (PH3) antibody in the whole midgut. We observed an increase in mitosis with a peak at 48 h PI although this effect was weaker than in flies fed with $10^8$ CFU (Fig. 2A). As it has been shown that Upd/JAK/STAT signaling is required in ISCs to stimulate their proliferation upon the ingestion of *Pe* or *Ecc* (Buchon et al., 2010; Jiang et al., 2009; Osman et al., 2012; Zhou et al., 2013), we tested whether this was also the case upon ingestion of small amounts of *Btk*. We blocked Upd/JAK/STAT signaling in ISCs by temporally expressing a dominant-negative form of the Upd receptor Dome ($Dome^{\Delta Cyt2\text{-}3}$) using the TARGET system (McGuire et al., 2003) with the $escargot^{ts}$ driver ($esg^{ts}$, expressed in ISCs and EBs; Micchelli and Perrimon, 2006) and fed these flies with small amounts of *Btk*. As expected, ISC proliferation was blocked (Fig. 2B) and no increase in *esg>GFP* cells was observed (Fig. S2A-D). Therefore, as for *Ecc* and *Pe*, Upd/JAK/STAT signaling is also required in ISCs to stimulate their proliferation upon ingestion of small amounts of *Btk*.

Because upon division ISCs give rise to EBs, we next followed the number of progenitor cells (ISCs+EBs) in the posterior midgut using the *esg-lacZ* or *esg>GFP* markers. A higher density of $esg^+$ cells was present from day 1 until day 4 PI (Fig. 2C,E-H″). However, at day 3 PI, many of the $esg^+$ cells no longer divided (Fig. 2A,C) and were already committed to EC differentiation. Indeed, those cells also expressed the EC marker *myo1A>GFP*, indicating that they correspond to early ECs (eECs) (Fig. 2G′,G″, yellow arrows). As eECs ($esg\text{-}lacZ^+$, $myo>GFP^+$) have not completed their endoreplication (Bardin et al., 2010), they are also recognizable by their smaller nucleus compared with old ECs ($esg\text{-}lacZ^-$, $myo>GFP^+$; Fig. 2G″ white arrowheads). It is noteworthy that the increase in $esg^+$ cells number at day 1 PI appeared 24 h before the peak of ISC division (compare Fig. 2C with 2A). This observation was reminiscent of previously published data showing that a pre-existing pool of latent EBs could quickly differentiate upon a local demand and before the onset of ISC proliferation, to give rise to late EBs/early ECs (Antonello et al., 2015; Buchon et al., 2010). Accordingly, there is a rise in EC number of about 20% between days 1 and 3 PI (Fig. 2D, red curve) but this affects neither the length nor the width of the gut (Fig. S3F,G). The number of enteroendocrine cells was unaffected (Fig. 2E′,F′,G′,H′; Fig. S2E). Moreover, the excess of ECs resulted in a disturbance of the midgut epithelium as illustrated by the formation of EC multilayers, a change of EC cell shape from hexagonal to round with an extended apical pole, and a significant reduction of the intestinal lumen (Fig. 2E-G″; Fig. S3A-C″,H). Nonetheless, epithelial polarity was maintained as illustrated by the proper positioning of different apico-basal markers (Fig. S3B-C″). Interestingly, this phenomenon was also observed upon ingestion of a small amount of *Ecc* (Figs S2F-J; S3D-E″). The gut recovered its cellular homeostasis and structure within 5 or 6 days after exposure to *Btk* or to *Ecc*, respectively (Fig. 2C,D,H-H″; Fig S2F-J). Therefore, our data show that ingestion of small amounts of opportunistic bacteria triggers an accelerated cell renewal program, which generates a transient accumulation of enterocytes in the posterior midgut.

### Early absence of cell death is responsible for EC accumulation

Whereas the ingestion of low amounts of bacteria promoted EC accumulation, flies fed with larger amounts of bacteria (*Btk* or *Ecc*) displayed an opposite phenotype, i.e. a decrease in EC density (Fig. 2D, gray curve), even though the number of mitotic ISCs and progenitor cells was higher than upon the ingestion of smaller amounts of bacteria (Fig. 2A,C) (Buchon et al., 2010). Therefore, we hypothesized that, although accelerating the cell renewal program at low bacterial doses, the brief passage of bacteria in the gut might not be sufficient to promote cell death. Thus, the addition of new ECs to the epithelium could lead to an excess of ECs.

We first verified that large amounts of *Btk* and *Ecc* are indeed capable of inducing cell death. As expected, $10^8$ CFU of *Btk* or *Ecc* significantly increased the number of apoptotic ECs (labeled by an anti-activated-Caspase 3 antibody) at day 1 PI compared with unchallenged flies (Fig. 3A,C; Fig. S4B) (Buchon et al., 2009b). About 12% of ECs were labeled by the anti-Casp3 antibody compared with 1.8% in unchallenged guts (Fig. S4E). Although there were fewer ECs at days 1, 2 and 3 PI than in unchallenged flies, at day 4 PI, the number of ECs was equivalent to that of unchallenged guts, indicating that the cell replenishment program had efficiently replaced dead ECs (Fig. 2D).

Development (2017) 144, 808-819 doi:10.1242/dev.142539

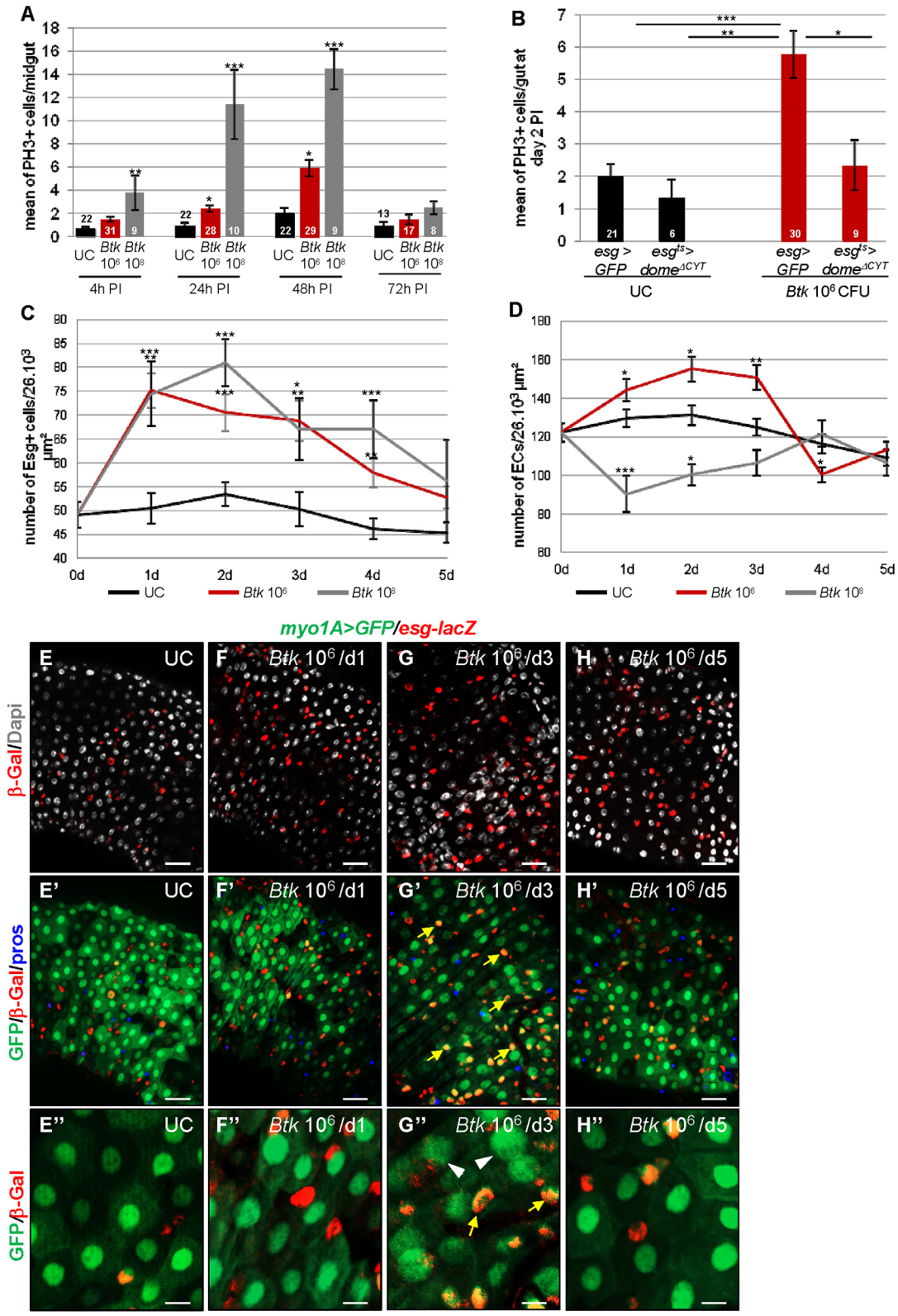


**Fig. 2. Mild stress induces ISC proliferation and an accumulation of enterocytes.** (A) Quantification of PH3$^+$ cells at 4, 24, 48 and 72 h PI in guts of flies fed with *Btk* $10^6$ CFU (red bars) and *Btk* $10^8$ CFU (gray bars) compared with those of unchallenged (UC; black bars) flies. (B) Quantification of PH3$^+$ cells in control midgut (*esg>GFP*) or in midgut expressing the dominant-negative form of the Upd receptor in progenitor cells (*esg$^{ts}$>dome$^{\Delta CYT}$*) 2 days after treatment with sucrose (UC; black bars) or *Btk* $10^6$ CFU (red bars). (C) Quantification of *esg*$^+$ cells from day 1 to day 5 PI in gut of flies fed with *Btk* $10^6$ CFU (red line) and *Btk* $10^8$ CFU (gray line) compared with unchallenged flies (UC; black line) ($10<n<46$). (D) Quantification of ECs from day 1 to day 5 PI in gut of flies fed *Btk* $10^6$ CFU (red line) or *Btk* $10^8$ CFU (gray line) compared with UC flies (black line). (E-H″) *myo1A>GFP, esg-lacZ* posterior midguts stained for the β-Gal (red), Pros (blue) and DNA (white) in midguts of UC flies (E-E″) and at days 1 (F-F″), 3 (G-G″) and 5 (H-H″) PI of *Btk* $10^6$ CFU-fed flies. Yellow arrows show eECs expressing both β-Gal and *myo>GFP* markers. White arrowheads indicate old ECs, which have bigger nuclei. Scale bars: 25 µm (E-H,E-H′); 7.8 µm (E″,F″,G″,H″).

Development (2017) 144, 808-819 doi:10.1242/dev.142539

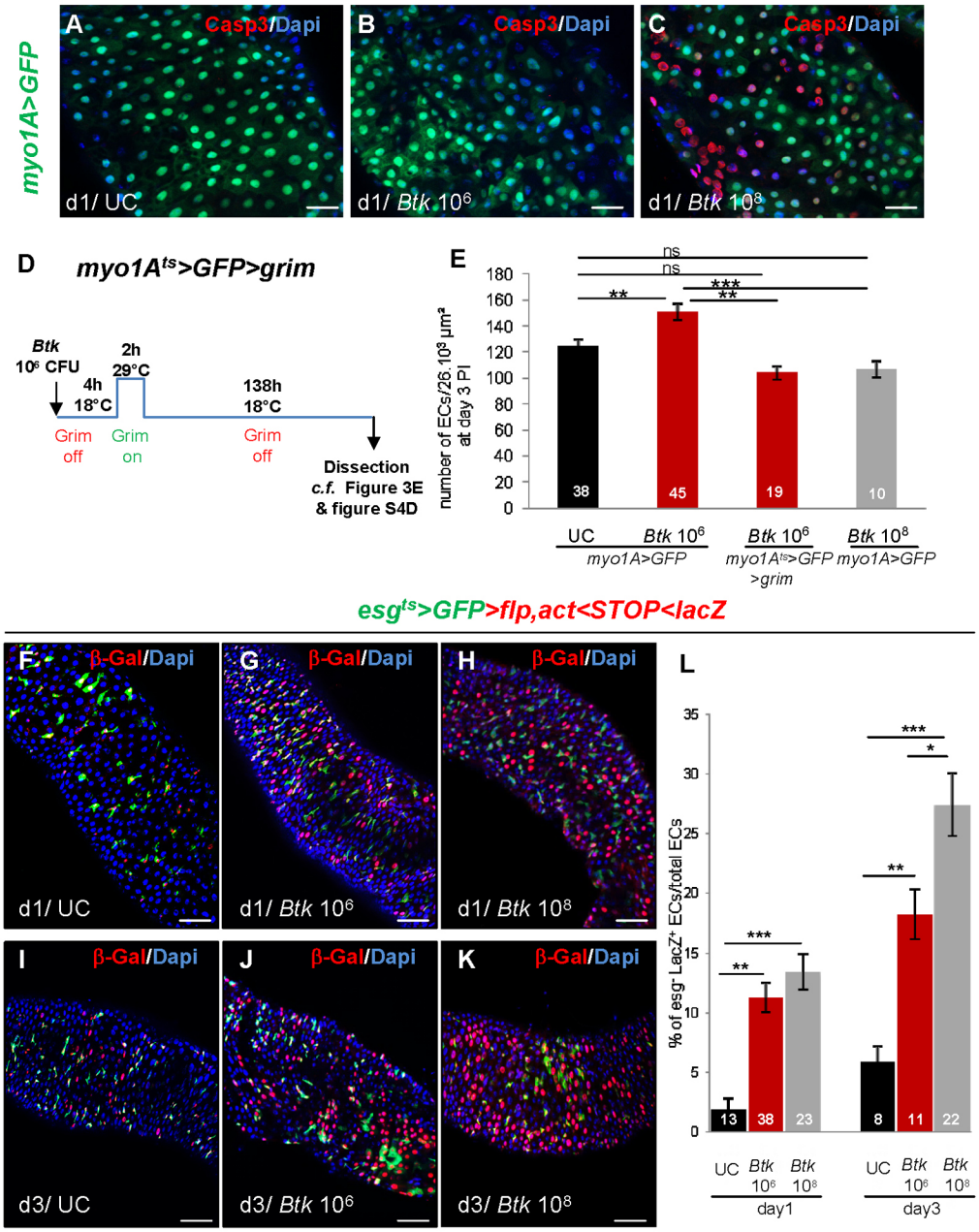


**Fig. 3. Early absence of cell death is responsible for EC accumulation.** (A-C) *myo1A>GFP* posterior midguts stained for Casp3 (red) and Dapi (blue) at day 1 PI. Flies were unchallenged (UC; A) or fed with *Btk* $10^6$ CFU (B) or *Btk* $10^8$ CFU (C). GFP marks the ECs. (D) Scheme of the experimental procedure for the transient expression of the pro-apoptotic gene *grim* in ECs. (E) Quantification of ECs at day 3 PI in UC, *Btk* $10^6$ CFU-fed, and *Btk* $10^8$ CFU-fed flies and in *Btk* $10^6$ CFU-fed flies overexpressing *grim*. (F-L) Cell lineage in *esg$^{ts}$>GFP >flp, act<CD2<lacZ* guts of flies fed with sucrose (UC) (F,I), *Btk* $10^6$ CFU (G,J), *Btk* $10^8$ CFU (H,K) at day 1 (F-H) and day 3 (I-K) PI. Guts are stained for β-Gal (red) and Dapi (blue). GFP marks the ISCs and EBs. (L) Percentage of newborn ECs. ns, not significant. Scale bars: 25 µm (A-C); 50 µm (F-K).

As expected, when flies were fed with $10^6$ CFU of *Btk* or *Ecc*, we did not detect any cell death during the first day (Fig. 3B; Fig. S4A,E). Therefore, if the excess of ECs was indeed due to the absence of cell death, inducing EC apoptosis genetically should suppress the supernumerary ECs. Using the TARGET system, we briefly expressed the pro-apoptotic gene *grim* specifically in ECs soon after ingestion of *Btk* and counted the number of ECs at day 3 PI (see schematic in Fig. 3D). In agreement, forced EC apoptosis (Fig. S4C) compensated for the lack of *Btk*-induced EC death and no excess of ECs was observed (Fig. 3E; Fig. S4D).

To confirm that the excess of ECs was indeed caused by the addition of newly formed ECs as well as the absence of early cell death, we marked all newborn ECs with β-galactosidase (β-Gal) antibodies from the time of *Btk* ingestion to the peak of EC number (at day 3) by combining the 'flip out' and TARGET systems. We then compared the percentage of marked ECs in guts from unchallenged, $10^6$ CFU- and $10^8$ CFU-fed flies at days 1 and 3 PI. In unchallenged flies, only 1.9% of ECs were marked after 1 day and about 6% were labeled at day 3 PI (Fig. 3F,I,L). We also observed that a little over 12 days were necessary to completely renew the gut epithelium (Fig. S4F-H′), which is consistent with previous estimates ranging between 12 (Jiang et al., 2009) and 21 (Antonello et al., 2015) days. In $10^6$ CFU-fed flies, 11.3% of ECs were labeled at day 1 and 18.2% at day 3 (Fig. 3G,J,L). As this percentage is close to the percentage of total EC increase (Fig. 2D), the excess of ECs can indeed be attributed to the addition of newborn ECs to the epithelium and the absence of early bacterial-induced apoptosis. In contrast, although the proportion of newborn ECs labeled at day 3 PI was much larger (almost 28%) in flies fed with $10^8$ CFU of *Btk* (Fig. 3H,K,L), the total number of ECs was reduced (Fig. 2D), demonstrating that the cell replenishment program is barely sufficient to overcome early-occurring EC death. Taken together, our results demonstrate that the excess of ECs observed during the 3 days following the ingestion of low

Development (2017) 144, 808-819 doi:10.1242/dev.142539

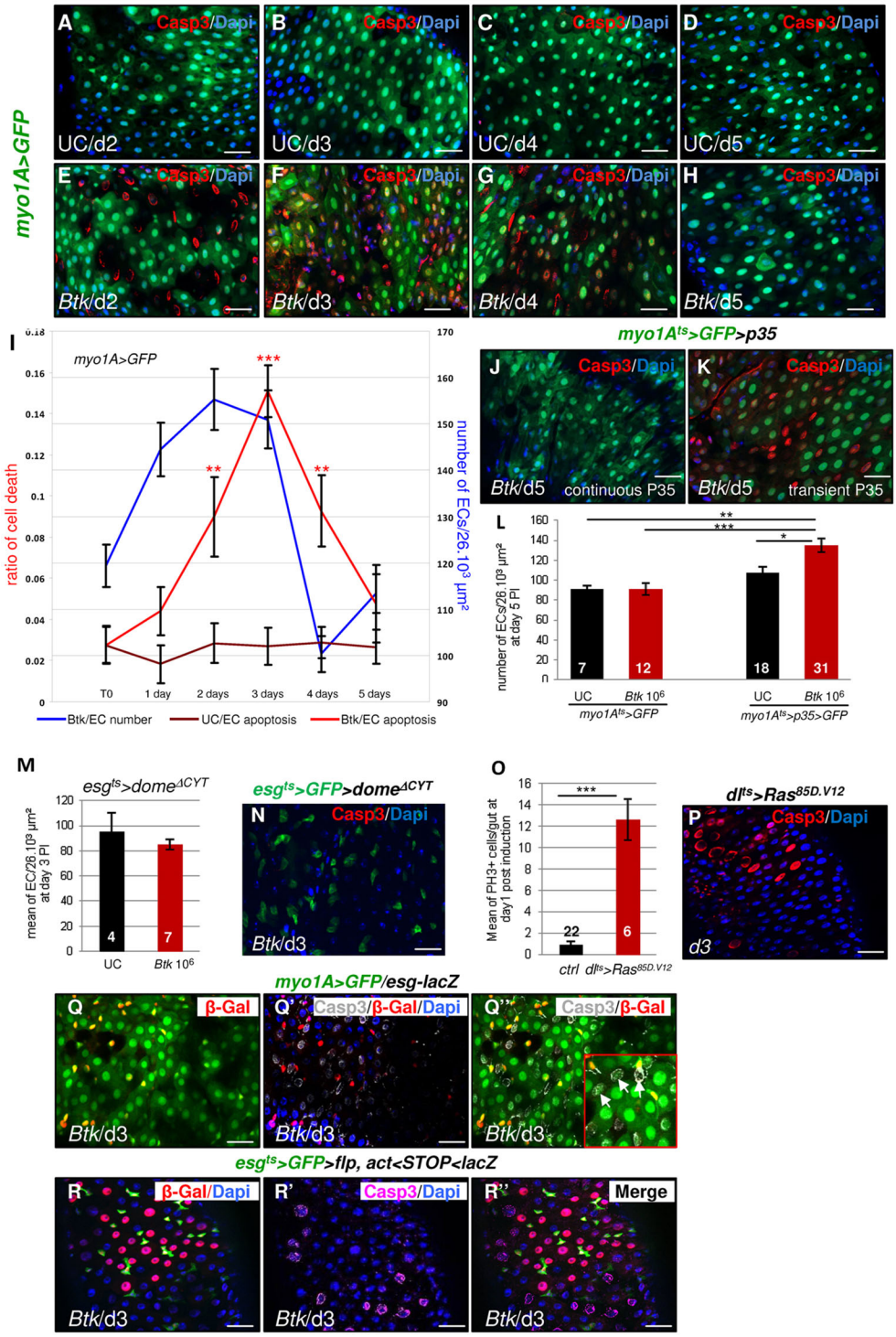


**Fig. 4. A wave of cell death eliminates supernumerary ECs.** (A-H) *myo1A>GFP* posterior midguts stained for Casp 3 (red) and Dapi (blue), 2 to 5 days PI of sucrose (UC) (A-D) or *Btk* $10^6$ CFU (E-H) treatment. (I) EC quantification in the posterior midgut of *Btk* $10^6$ CFU-fed flies (blue line) and ratio of apoptosis in UC flies (dark red line) and *Btk* $10^6$ CFU-fed flies (bright red line) from day 1 to day 5 PI. (J, K) *myo1A$^{ts}$>GFP>p35* posterior midguts of flies fed with *Btk* $10^6$ CFU in which the apoptosis was continuously (from days 2 to 5 PI) (J) or transiently (during day 2 PI) (K) inhibited by p35. Guts are labeled for Casp3 (red) and Dapi (blue). GFP marks the ECs. (L) EC quantification 5 days PI in *myo1A$^{ts}$>GFP* and *myo1A$^{ts}$>GFP>p35* posterior midguts from flies fed with sucrose (UC) or *Btk* $10^6$ CFU. (M) EC quantification 3 days PI in *esg$^{ts}$>GFP>dome$^{\Delta CYT}$* (previously transferred at 29°C for 4 days) posterior midguts of flies fed with sucrose (UC) or *Btk* $10^6$ CFU. (N) *esg$^{ts}$>GFP>dome$^{\Delta CYT}$* posterior midguts labeled for Casp3 (red) and Dapi (blue) 3 days PI. (O) Quantification of $PH3^+$ cells 1 day after the induction (2 h at 29°C) of *Ras$^{85D.V12}$* expression in *dl$^{ts}$> Ras$^{85D.V12}$* midguts (red bar) compared with control midguts (ctrl, black bar). (P) *dl$^{ts}$> Ras$^{85D.V12}$* posterior midguts labeled for Casp3 (red) and Dapi (blue) 3 days post induction of *Ras$^{85D.V12}$*. (Q-Q″) *myo1A*>GFP, *esg-lacZ* posterior midguts of *Btk* $10^6$ CFU-fed flies, stained for β-Gal (red), Casp3 (white) and Dapi (blue) at day 3 PI. GFP marks the ECs. eECs are yellow (β-Gal$^+$; GFP$^+$). White arrows point to apoptotic ECs (β-Gal$^-$; GFP$^+$). (R-R″) *esg$^{ts}$>GFP>flp, act<STOP<lacZ* posterior midguts stained for β-Gal (red), Casp3 (pink) and Dapi (blue) 3 days PI of *Btk* $10^6$ CFU. Note that the Casp3 staining never marks the newborn ECs (red nuclei). Scale bars: 30 µm.

amounts of opportunistic bacteria is due to the induction of a mild cell renewal program in the absence of bacteria-induced cell death.

### A late wave of cell death eliminates supernumerary ECs

We then investigated how the midgut resorbs the excess of ECs to return to its homeostatic state. One efficient mechanism to return to homeostasis could be the elimination of supernumerary ECs by apoptosis. We therefore monitored apoptosis from the day following the intoxication by $10^6$ CFU of *Btk* up until midgut recovery. No cell death was observed at 1 day PI as mentioned above (Fig. 3B). However, we started to detect apoptotic ECs during day 2 PI, with a peak at day 3 PI. EC apoptosis then decreased during day 4 PI and had disappeared by day 5 PI (Fig. 4A-I). To demonstrate that EC apoptosis is required to restore cellular homeostasis of the posterior midgut, we blocked EC death (using the anti-apoptotic p35 factor) from day 2 PI onwards and checked whether the excess of ECs was maintained. As expected, whereas control midguts had regained their normal cell density by day 5 PI (Fig. 4H,L), midguts in which cell death had been blocked still displayed an excess of ECs (Fig. 4J,L; Fig. S5A). We also noticed that inhibiting EC death in unchallenged

Development (2017) 144, 808-819 doi:10.1242/dev.142539

flies slightly increased (although not significantly) the number of ECs (Fig. 4L, UC *myo1A$^{ts}$>p35>GFP*), mostly reflecting the inhibition of naturally occurring cell death (Fig. 4I, dark red). We further transiently blocked apoptosis during day 2 PI (according to the protocol in Fig. 5B). As expected, EC apoptosis was blocked at day 3 PI associated with an excess of ECs (Fig. S5B). Interestingly,

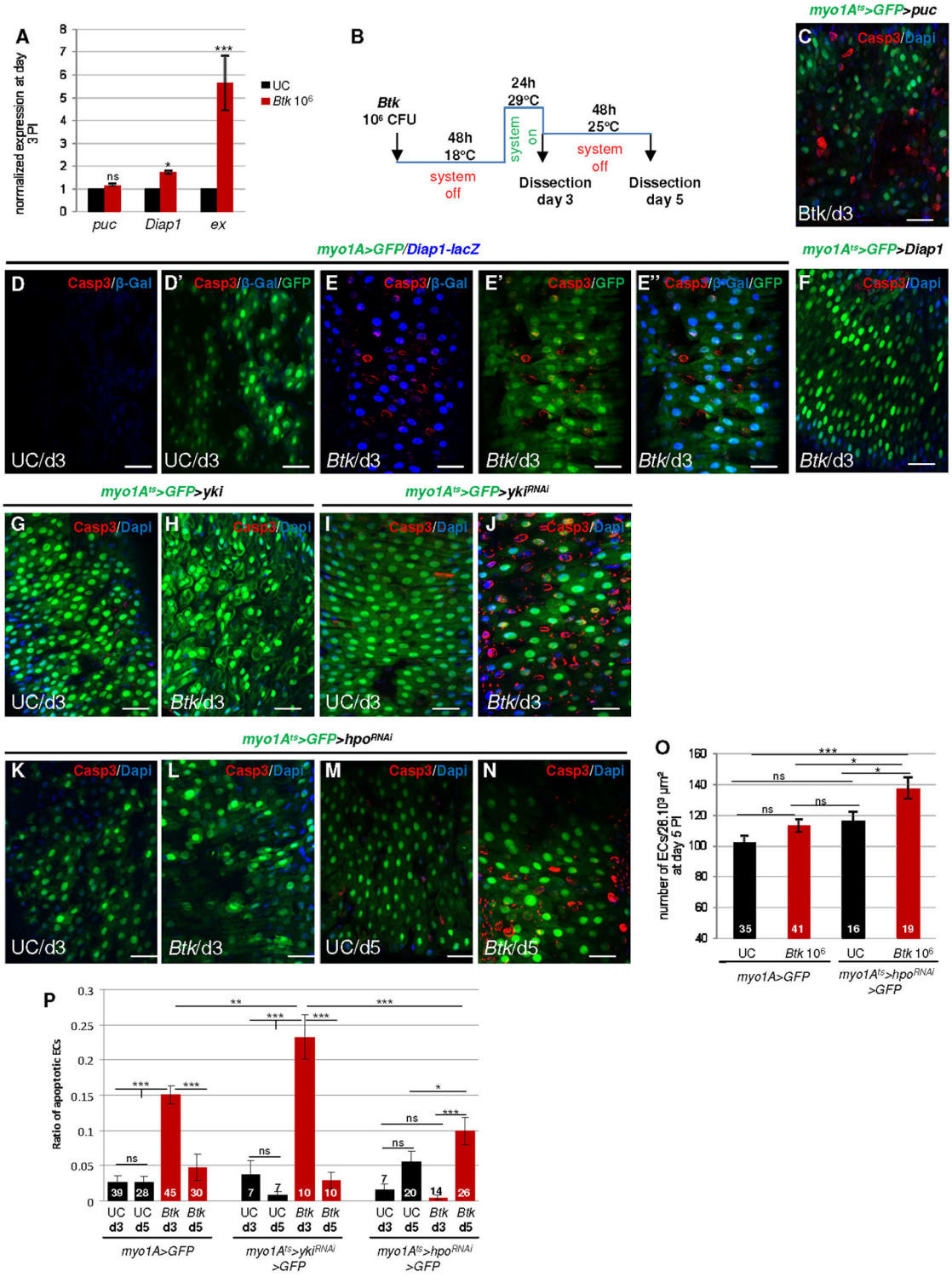


**Fig. 5. Hpo is involved in EC apoptosis in response to their excess**. (A) RT-qPCR at day 3 PI on midguts of flies fed with sucrose (UC) or *Btk* $10^6$ CFU ($n$=30). (B) Scheme of the experimental procedure for transient expression in the ECs (using the *myo1A$^{ts}$* driver) of *puc* (C), *Diap1* (F), *yki* (G,H), *yki$^{RNAi}$* (I,J) and *hpo$^{RNAi}$* (K-N). (C) *myo1A$^{ts}$>GFP>puc* posterior midgut of fly fed with $10^6$ CFU of *Btk* 3 days PI. (D-E″) *myo1A>GFP, Diap1-lacZ* posterior midguts of flies fed with sucrose (D,D′) or $10^6$ CFU of *Btk* (E-E″) 3 days PI. GFP marks the ECs. Casp3 (red) and β-Gal (blue). (F-N) *myo1A$^{ts}$>GFP* posterior midguts of flies fed with sucrose (G,I,K,M) or $10^6$ CFU of *Btk* 3 days PI (F,H,J,L) or 5 days PI (N), and overexpressing *Diap1* (F), *yki* (G,H), *yki$^{RNAi}$* (I,J), or *hpo$^{RNAi}$* (K-N). (O) Quantification of ECs at day 5 PI in UC and *Btk*-fed *myo1A>GFP* flies (left) and *myo1A$^{ts}$>GFP>hpo$^{RNAi}$* flies (right). (P) Ratio of apoptosis in posterior midguts at days 3 and 5 days PI in UC and $10^6$ CFU *Btk*-fed *myo1A>GFP* flies (left), *myo1A$^{ts}$>GFP>yki$^{RNAi}$* flies (center) and *myo1A$^{ts}$>GFP>hpo$^{RNAi}$* flies (right). ns, not significant. Scale bars: 30 µm.

Development (2017) 144, 808-819 doi:10.1242/dev.142539

EC apoptosis was delayed, only peaking at day 5 PI (i.e. once the inhibition had faded) (Fig. 4K). Hence, apoptosis is indeed the mechanism employed for the elimination of supernumerary ECs. To confirm that the wave of apoptosis was specific to the excess of ECs and not due to residual opportunistic bacteria remaining in the gut, we monitored the occurrence of apoptotic cells 3 days PI in $esg^{ts}>Dome^{\Delta Cyt2\text{-}3}$ flies fed with low amounts of *Btk*. In these flies there was neither ISC proliferation (Fig. 2B) nor accumulation of ECs (Fig. 4M). Consequently, we did not observe any apoptotic cell 3 days PI (Fig. 4N).

We then wondered whether genetically inducing an excess of ECs would also trigger a wave of apoptosis to remove supernumerary ECs. To explore this possibility, we used the ISC-specific driver *delta-Gal4* to transiently express the $Ras^{85D.V12}$ oncogenic allele ($dl^{ts}> Ras^{85D.V12}$). A pulse of 1 h of $Ras^{85D.V12}$ expression in ISCs was sufficient to promote ISC proliferation as highlighted by the increase in the mitotic PH3 labeling (Fig. 4O). Interestingly, we observed a wave of apoptosis at day 3 (Fig. 4P) demonstrating that apoptosis is a physiological mechanism required to remove supernumerary ECs whatever the cause of their excess.

Finally, we investigated whether the wave of EC death removed ECs randomly or selectively (i.e. the newborn ones and/or the old ones). To do so, we took advantage of the perdurance of the β-Gal labeling and used a *Drosophila* line in which eECs are co-labeled by *esg-lacZ* and *myo1A>GFP* markers. Strikingly, we observed that at day 3 PI, dying ECs were never β-Gal$^+$ (i.e. eECs; Fig. 4Q-Q″). On the contrary, the Casp3 staining mainly marked old ECs recognizable by their large nuclei and their GFP labeling (Fig. 4Q′,Q″). We confirmed this result using the lineage tracing 'flip out'/TARGET system, which labels all newborn ECs with β-Gal. Consistently, dying ECs were unmarked by β-Gal and had large nuclei, hence dying ECs were mainly old ECs (Fig. 4R-R″). Together, our results demonstrate that following the induction (physiological or genetical) of an excess of ECs, the midgut returns to its cellular homeostasis by triggering a wave of EC death that selectively removes old ECs.

### Hpo is involved in EC apoptosis in response to their excess

In order to gain further insight into the physiological process triggering cell death, we searched for the signaling pathways that might sense the supernumerary ECs and promote the wave of EC death. The JNK and/or Hpo/Yki pathways appeared to be good candidates due to their known implication in the control of apoptosis (Igaki, 2009; Yu and Guan, 2013).

The JNK pathway was quickly ruled out because (1) the JNK target gene *puc* was not induced at the time of the wave of cell death (e.g. at days 1 and 3 PI; Fig. 5A; Fig. S1G; Fig. S6A) and (2) overexpressing the JNK inhibitor Puc in ECs at day 2 PI (according to the protocol in Fig. 5B) did not inhibit EC death at day 3 PI (Fig. 5C). On the contrary, the Yki target genes *Diap1* and *ex* were induced at day 3 (Fig. 5A), as confirmed using *Diap1-lacZ* (Fig. 5D-E) and *ex-lacZ* (Fig. S6B,C) reporter genes. Remarkably, *Diap1*, which encodes an anti-apoptotic factor, was strongly expressed in non-apoptotic ECs (Fig. 5E-E″). We observed a similar *ex-lacZ* expression in non-dying cells (Fig. S6D-E″). Overexpressing either Diap1 or Yki in ECs during day 2 PI (according to the protocol in Fig. 5B) inhibited EC apoptosis during the third day (Fig. 5F-H). These data suggest that Hpo activation in ECs might indeed be responsible for inducing apoptosis of supernumerary ECs by inhibiting Yki activity in cells destined to die. Hence, we first silenced *yki* expression in all ECs during day 2 PI and monitored apoptosis at day 3 PI (according to Fig. 5B). As expected, in *yki*-depleted guts, the ingestion of small amounts of *Btk* drastically increased EC apoptosis at day 3 PI compared with wild-type *Btk*-fed flies or unchallenged flies (Fig. 5J compared with Fig. 5I and Fig. 4F; Fig. 5P). It is noteworthy that in unchallenged guts, transient depletion of *yki* in the ECs did not significantly increase their apoptosis (Fig. 5I,P). We then transiently silenced *hpo* expression in ECs at day 2 PI (according to Fig. 5B). Consistently, cell death was abolished at day 3 PI (Fig. 5K,L,P). Moreover, the excess of ECs was maintained and the wave of cell death was postponed to day 5 PI (Fig. 5M-P). Furthermore, continuous silencing of *hpo* completely inhibited EC death up until day 5 PI (Fig. S6F). To confirm this result, we used the 'flip out' system to randomly and briefly silence *hpo* expression in the midgut epithelial cells during day 2 PI. In this case, EC apoptosis was observed exclusively in the tissue surrounding *hpo*-depleted cells (Fig. S6G-G″). We confirmed the requirement of Hpo signaling by transiently silencing *salvador* (*sav*, encoding the binding partner of Hpo; Fig. S6H,I). Finally, we performed an epistasis test to show that indeed Hpo is involved in the wave of apoptosis through the inhibition of Yki activity by transiently knocking down the expression of both *hpo* and *yki* in ECs (according to the protocol in Fig. 5B). As expected, a wave of cell death occurred at day 3 PI (Fig. S6J,L) and the gut recovered its cellular homeostasis by day 5 PI (Fig. S6K,L). Taken together, our data strongly suggest that activation of Hpo signaling acts autonomously in ECs to trigger the wave of apoptosis necessary to remove the supernumerary ECs induced by the ingestion of small amounts of opportunistic bacteria.

### Physiological consequences

To complete our study, we assessed the functional impacts that the ingestion of low amounts of *Btk* may have knowing that bacterial intoxication, cell death or the presence of too many immature cells in the gut can affect its digestive functions (Biteau et al., 2008; Buchon et al., 2009b; Chakrabarti et al., 2012; Dutta et al., 2015; Erkosar et al., 2015). Therefore, we monitored several metabolic and enzymatic parameters in the midgut. A reduction of EC lipid storage appeared by day 2 PI (Fig. 6A,B) which correlated with a lower expression of *lipaseA* (*lipA*; *magro* – FlyBase), which regulates lipid absorption by ECs) at day 1 PI (Fig. 6C) (Karpac et al., 2013). At day 3 PI, *lipA* expression increased again, probably compensating for the impaired lipid absorption during the previous days. We also noticed a decrease in *trypsin ε* expression and trypsin activity (Fig. 6D,E) (Biteau et al., 2008) that may result in impaired protein digestion. Of note, we did not observed any changes in food intake (Fig. 6F). Because flies overcame acute food poisoning without any mortality (data not shown), we wondered whether chronic ingestion of low amounts of *Btk* bacteria could affect fly longevity. Based on the fact that the gut needs 5-6 days PI to regain homeostasis, we provided flies with small amounts of bacteria once a week during all their life and further monitored their longevity. Under such chronic intoxication, fly longevity appeared to be reduced by almost 24% (Fig. 6G). Thus, our results indicate that acute ingestion of small amounts of opportunistic bacteria, although apparently inoffensive, transiently affects the digestive and absorptive functions of the gut and, in the long run, chronic ingestion reduces lifespan.

## DISCUSSION

### Cell renewal versus cell replenishment

In this study, we highlighted a physiological mechanism accelerating cellular gut renewal that probably occurs more frequently than the gut replenishment required after a widespread cell death. Indeed, animals as well as humans are more likely to be

Development (2017) 144, 808-819 doi:10.1242/dev.142539

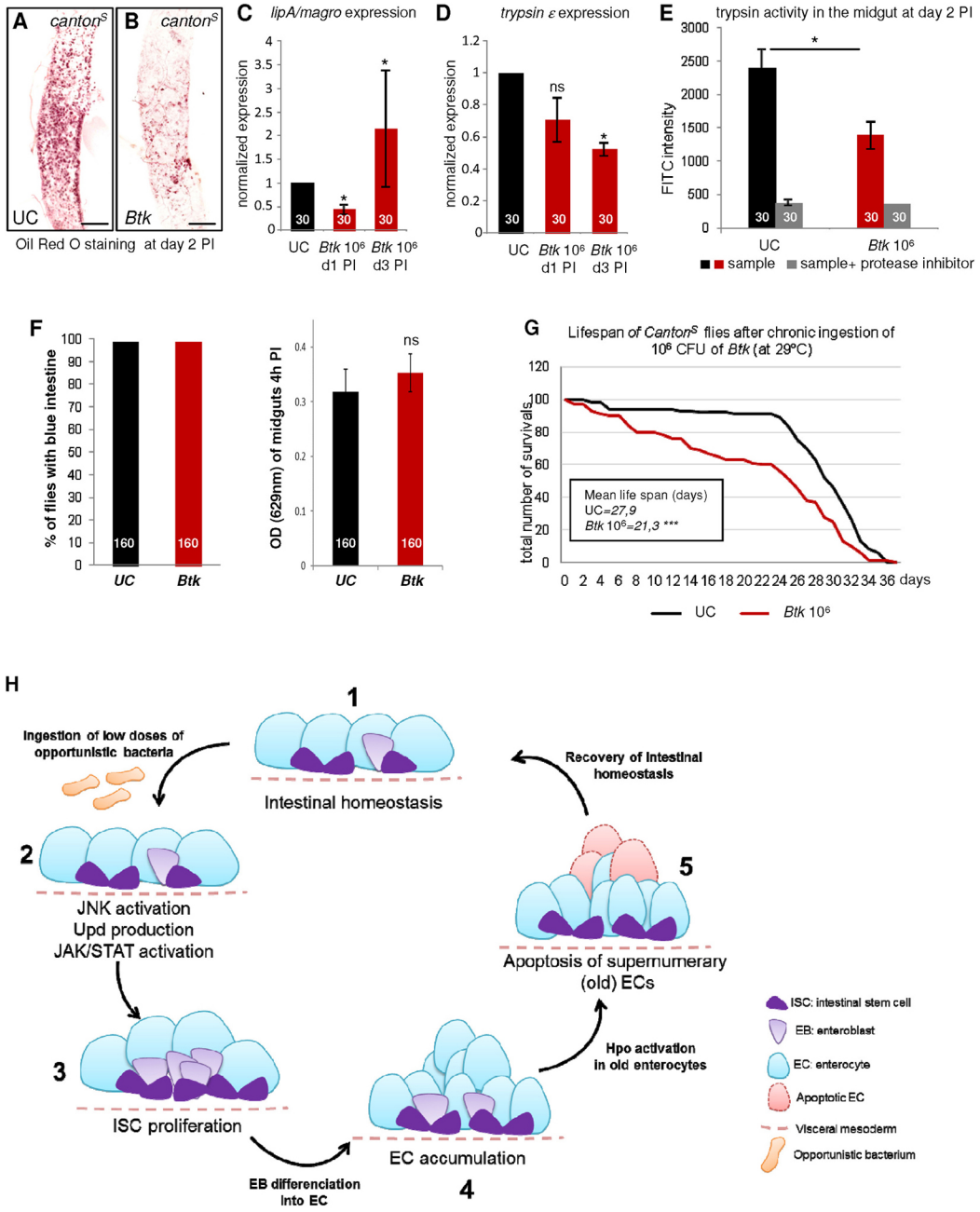


**Fig. 6. Physiological consequences.** (A,B) Posterior midguts of Canton$^S$ flies stained with Oil Red O at day 2 PI show reduced lipid accumulation in ECs of flies fed with *Btk* $10^6$ CFU ($n$=30). Scale bars: 100 µm. (C,D) RT-qPCR on midguts from flies fed with sucrose (UC) or $10^6$ CFU of *Btk* at day 1 and day 3 PI. (E) Measurement of trypsin activity (proportional to FITC intensity) in midguts from flies fed with sucrose (UC) or with *Btk* $10^6$ CFU 2 days PI. There is a reduction of about 42% of trypsin activity following *Btk* treatment. (F) Food intake 4 h PI in Canton$^S$ flies fed with sucrose (UC) or *Btk* $10^6$ CFU. The food is dyed using Erioglaucine Blue. Left: percentage of flies having ingested colored food. Right: Erioglaucine Blue $OD_{629}$ measured in the intestine. (G) Lifespan of Canton$^S$ flies at 29°C after chronic intoxication with sucrose (UC; black line) or with *Btk* $10^6$ CFU (red line) ($n$=100). (H) Model of the physiological control of gut integrity upon ingestion of low amounts of opportunistic bacteria. The ingestion of small amounts of opportunistic bacteria along with food induces moderate JNK and JAK/STAT signaling activation in ECs and ISCs, respectively (2). During the first 48 h, the mild increase in ISC proliferation generates EBs (3). During days 1 to 3 post ingestion, EB differentiation generates too many ECs, resulting in an excess of ECs (4). Hpo signaling activation (Yki off) in old ECs leads to their apoptosis, enabling the elimination of the supernumerary ECs (5), allowing the gut to recover its cell homeostasis (1). ns, not significant.

subject to the ingestion of low levels of opportunistic bacteria than to the ingestion of virulent pathogens or high levels of opportunistic bacteria. Upon ingestion of small amounts of bacteria, a cell renewal program is launched in spite of the fact that the ingested bacteria are rapidly eliminated from the gut without promoting any cell death. Our data demonstrate that ISC division is stimulated, but to a lesser extent than that triggered by pathogens or harmful chemicals that promote widespread cell death (Amcheslavsky et al., 2009; Apidianakis et al., 2009; Buchon et al., 2009a; Chakrabarti et al., 2012; Chatterjee and Ip, 2009; Cordero et al., 2012; Jiang et al., 2009, 2011; Karpowicz et al., 2010; Ren et al., 2010, 2013; Staley and Irvine, 2010). Interestingly, the switch from accelerated cell renewal to cell replenishment appears to be correlated with activation of Hpo/Yki signaling. Indeed, we showed that small

Development (2017) 144, 808-819 doi:10.1242/dev.142539

amounts of opportunistic bacteria briefly activate JNK signaling and do not promote cell death. Consequently, the mild induction of *upd* genes leads to an increase in cell renewal. Because of the absence of cell death, there is an excess of ECs (Fig. 6H). Upon a stronger aggression, there is a sustained activation of JNK signaling pathway (our work) (Buchon et al., 2009a) inducing apoptosis. Knowing that (1) cells destined to die rapidly change their adhesive properties with their neighboring cells (Taylor et al., 2008) and (2) Hpo/Yki signaling pathway is sensitive to cell-cell contact (Boggiano and Fehon, 2012), we propose that upon a strong aggression, the rapid EC engagement towards apoptosis promotes changes in cell adhesion that repress Hpo, inducing Yki activities. This model is supported by the absence of Yki target gene activation by *Pe* when JNK signaling is abolished (Fig. 1C). In agreement, it was previously shown that activation of the JNK pathway is able to induce Yki target gene expression to levels comparable to ours (Shaw et al., 2010). It has also been shown that overexpression of the JNKK (Hep) in ECs promotes nuclear Yki localization (Staley and Irvine, 2010). Consequently, the concomitant activation of JNK and Yki strongly activates their common target genes, such as *upd* cytokines. Those cytokines will non-autonomously induce ISC proliferation and differentiation to quickly replace the dying ECs. Therefore, the huge production of cytokines and growth factors is probably required to accelerate the rate of ISC proliferation rather than to trigger ISC proliferation per se. Switching from a cell renewal program to a cell replenishment program is probably necessary for an efficient replacement of the dying cells to maintain gut integrity upon huge damages.

### Maintenance of cell density in the gut

In this study, we showed that excess of ECs, whatever is its origin, is rapidly overcome and the gut recovers its normal EC number in less than a week thanks to a wave of apoptosis. This phenomenon presents similarities with the adaptation of gut size to nutrient availability. Indeed, whereas feasting stimulates gut growth, subsequent fasting for several days induces widespread apoptosis to reduce the size of the gut (O'Brien et al., 2011). This is also reminiscent of what happens during *Drosophila* eye development where the Hpo pathway controls the final size of the differentiating organ by inducing cell death to remove unspecified supernumerary inter-ommatidial cells (Kango-Singh and Singh, 2009). As we found that the Hpo pathway was involved in triggering the wave of apoptosis to remove the supernumerary ECs, our data show that a mechanism used during development can be reused during adulthood to facilitate the removal of extra cells and restore gut integrity (Fig. 6H). Moreover, in many vertebrate cell culture studies, Yki/Yap and Hpo signaling are involved in the sensing of cell morphology and density (Gaspar and Tapon, 2014). At low density, cells spread and Yki/Yap is nuclear, promoting cell proliferation. At higher density, cells are rounder and smaller, Yki/Yap is cytoplasmic and proliferation is halted (Ota and Sasaki, 2008; Varelas et al., 2010; Zhao et al., 2007). Therefore, we assume that the implication of Hpo signaling in triggering the wave of apoptosis to remove supernumerary ECs could be due to both a change in EC shape and an increase in their density (Fig. 6H). Indeed, we observed at day 1 PI that the density of EC was higher and their shape become rounder. Taken together, these modifications can activate Hpo signaling leading to Yki inhibition and to the death of supernumerary ECs. This preferentially occurs in old ECs because they are probably more susceptible to cell shape change. Indeed, old ECs begin to die at day 2 whereas eECs are not yet fully differentiated. Moreover, as ISCs are basally located in the gut epithelium; when the new eECs arise, the old ones are pushed towards the lumen facing the putative aggressors, thus protecting the new ones. Once the aggression is resolved, the old ECs (that may be damaged) are eliminated, leaving the new ones intact.

Finally, it is increasingly thought that the ingestion of bacteria might trigger or exacerbate inflammatory bowel diseases and/or colorectal cancer (Collins et al., 2011; Tjalsma et al., 2012). Our work thus brings new insight into the understanding of the mechanisms and signaling pathways that might be involved in those pathologies upon ingestion of opportunistic bacteria along with the food.

## MATERIALS AND METHODS

### Bacterial strains

The *Btk* strain (identified under the code 4D22) was provided by the Bacillus Genetic Stock Center (www.bgsc.org) and described by González et al. (1982). *Ecc* and *Pe* were kindly provided by Bruno Lemaitre's laboratory (École Polytechnique Fédérale, Lausanne, Switzerland). *L. plantarum* was kindly provided by Bernard Charroux (IDBM, Marseille, France). *Pe*, *Btk* and *Ecc* were grown in LB medium at 30°C for 16 h and *L. plantarum* was grown in MRS medium (de Man, Rogosa and Sharpe medium; Sigma, 69964) for 16 h in anaerobic conditions at 37°C.

### Fly strains

For details of fly strains used, see supplementary Materials and Methods.

### Bacteria counting

Flies were fed with *Btk* and *L. plantarum*, washed with ethanol and distilled water before dissection of the guts in PBS. Guts were crushed in 200 µl of LB (Luria–Bertani medium; Fisher BioReagents, BP1426-2) or MRS medium at various times after intoxication using a micropestle, and the homogenate was serially diluted in LB or MRS medium and incubated overnight at 30°C (*Btk*) or 37°C (*L. plantarum*).

### *Drosophila* rearing, intoxication and longevity

*Drosophila* were reared on standard medium at 25°C unless otherwise mentioned. For oral intoxication, after 2 h of starvation, 3- to 5-day-old virgin females (at 25°C) were flipped onto fly medium covered with filter disks soaked in a 1:1 mix of bacterial pellets and 5% sucrose (concentrations of bacteria used: 1.106 CFU/5 $cm^2$/fly or 1.108 CFU/5 $cm^2$/fly). Flies were kept to feed on the contaminated media until dissection in all the experiments. For lifespan experiments, 3- to 5-day-old (at 25°C) virgin females were fed with 5% sucrose (UC, unchallenged) or *Btk* at 106 CFU/5 $cm^2$/fly and were weekly flipped onto new contaminated fly medium. The lifespan experiments were performed at 29°C.

### Dissection, immunostaining and microscopy

Dissection, fixation and immunostaining were performed as described by Micchelli (2014). Dilutions of the various antibodies were: mouse anti-Prospero at 1:200 [Developmental Studies Hybridoma Bank (DSHB)], mouse anti-β-Gal at 1:500 (Promega, Z3781), rabbit anti-β-Gal at 1:1000 (Cappel, 55976), rabbit anti-PH3 at 1:1000 (Millipore, 06-570), rabbit anti-Casp3 at 1:300 (Cell Signaling, 9661), mouse anti-Arm at 1:100 (DSHB), Cy3 anti-mouse at 1:1000 (Jackson ImmunoResearch, 715-165-150), Cy3 anti-rabbit at 1:1000 (Jackson ImmunoResearch, 101394), Cy5 anti-rabbit at 1:300 (Jackson ImmunoResearch, 111-175-144), Alexa647 anti-mouse at 1:500 (Invitrogen, A21235) and Phalloidin-Alexa555 at 1:1000 (Molecular Probes, A34055). For microscopy, guts were mounted in Fluoroshield-DAPI medium (Sigma) and immediately observed on a Zeiss Axioplan Z1 with Apotome 2 microscope. Images were analyzed using ZEN (Zeiss), ImageJ and Photoshop software. Image acquisition was performed on the Microscopy Platform of the Institut Sophia Agrobiotech (INRA 1355-UNS-CNRS 7254-Sophia Antipolis).

### RT-qPCR

Total RNA was extracted from ten midguts with Trizol reagent (Invitrogen) and dissolved in 20 µl of RNase-free water. cDNA was then synthesized from 550 ng total RNA and qPCR was carried out using an AriaMX real-Time PCR System (Agilent) and the EvaGreen kit (Euromedex). Each

Development (2017) 144, 808-819 doi:10.1242/dev.142539

experiment was independently repeated three times. Moreover we performed three technical repeats. Relative expression data were normalized to *Rp49* (*RpL32* – FlyBase) and *Dp1* genes. See Table S1 for primer sequences.

### Measurement, counting and statistical analysis

In all the data presented, the pictures and counting were always done in the posterior part of the R4 region (http://flygut.epfl.ch/histo_regions/9) named R4bc in the flygut site (see also Buchon et al., 2013 and Marianes and Spradling, 2013). Experiments were independently repeated at least three times. Cells were counted in a fixed area (26.103 µm²) within the R4bc region. For EC counting in the Fig. 2D and Fig. 4I, we considered a cell to be a 'true' EC only when it was expressing the myo1A>GFP marker, meaning that dying ECs that no longer expressed the GFP and differentiating EBs that did not yet express the GFP were omitted. The numbers within the bars of all the graphs correspond to the number of guts analyzed. Results are presented as mean±s.e.m. Effects of treatments were analyzed using a pair wise comparison test (Tukey's test). Differences were considered significant when $P<0.05$ ($*P\leq0.05$, $**P\leq0.01$, $***P\leq0.001$).

### Frozen sections

Posterior midguts were incubated with antibodies as described above, frozen in OCT medium and cut with a Leica M3050-S Microtome into 10 µm frozen sections to obtain transversal sections of posterior midguts. Sections were then mounted in Fluoroshield-DAPI medium before observation.

### Flip-out clones

For flip-out clones, *y w hs-flp; UAS-hpo$^{RNAi}$* females were crossed with *w; act<CD2<Gal4;UAS-GFP* males at 18°C. Progeny was transferred to bacteria supplemented media at 18°C for 48 h, then heat-shocked for 45 min at 37°C before being transferred to 25°C and dissected after 24 h.

### Cell lineage

*w; esg-Gal4 UAS-GFP; tubGal80$^{ts}$* females were crossed with *w; act<STOP<lacZ; UAS-flp* males at 18°C. Progeny were kept for 6-8 days at 18°C. Then, the progeny were transferred to sucrose (Fig. 3F,I; Fig. S4F-H′) or bacteria-supplemented media (Fig. 3G,H,J-L; Fig. 4R-R″) at 29°C for 1 day, 3 days and 12 days.

### Oil Red O lipid staining

The protocol was adapted from Karpac et al. (2013) with minor changes: guts were fixed for 40 min and incubation time with Oil Red O solution was 45 min.

### Protease activity

Eight intestines were crushed in 50 µl PBS, then spun at 10,000 ***g*** for 5 min at 4°C. The supernatant was kept and diluted at 1/10. Then protease activity was measured using Protease Fluorescent Detection Kit (Sigma): 5, 10 and 20 µl of diluted samples were added to 10 µl of 10× PBS, 20 µl of FITC-Casein and 70 µl of distilled water (control experiment was performed with trypsin at 10 mg/ml in 1 mM HCl). The tubes were gently mixed and incubated at 37°C for 90 min, then 300µl of 10% TCA added. Mixes were incubated at 37°C for 30 min, then spun for 10 min at 13000 rpm (10,000 ***g***) at 4°C and 50 µl of the resulting supernatant was added to 150 µl of 1 M Tris pH 8.5. The fluorescence of the sample was measured at 535 nm.

### Food intake

Virgin females (3 to 5 days old; 25°C) were transferred into blue-colored food [the final concentration of the erioglaucine disodium salt blue dye (Sigma-Aldrich) was 0.75%] mixed with sucrose (UC) or with 1.106 CFU of *Btk*. Four hours post-ingestion, flies with blue intestine were counted and then dissected. Ten intestines per 2 ml tube were collected and rapidly frozen. Then the guts were crushed using a 5 mm steel bead in a Tissue Lyser for 2 min at 50 Hz. The guts were spun for 3 min at 10,000 ***g*** at 4°C. The optic density of the supernatant was measured at 629 nm with a Nanodrop.

#### Acknowledgements

We are grateful to N. Tapon, J Colombani, R. Rousset, T. Adachi-Yamada, T. Ip, M. Kango-Singh, S. Hou, X. Zeng, Y. Apidianakis, C. Micchelli and D. Osman for fly stocks. We also thank N. Arquier for the food intake protocol. We also would like to thank R. Delanoue, J. Colombani and R. Rousset for constructive discussions and for critical analysis of the manuscript. We thank the Microscopy Platform of the Institut Sophia Agrobiotech (INRA 1355- UNS - CNRS 7254, Sophia Antipolis) for access to instruments.

#### Competing interests

The authors declare no competing or financial interests.

#### Author contributions

R.L. contributed to conception and design, acquisition of data, analysis and interpretation of data, revising the article; A.B.-B., O.B., M.-P.N.-E. and M.A. contributed to acquisition of data; D.P. contributed to acquisition of data and revising the article; A.G. contributed to conception and design, drafting and revising the article.

#### Funding

This work was supported by a grant from the MESR (Ministère de l'Education Nationale, de l'Enseignement Superieur et de la Recherche) (R.L.), the Fondation pour la Recherche Médicale (R.L.), the Institut National de la Recherche Agronomique, the Centre National de la Recherche Scientifique, and the Agence Nationale de la Recherche (ANR-13-CESA-0003-01 to A.G.).

#### Supplementary information

Supplementary information available online at
http://dev.biologists.org/lookup/doi/10.1242/dev.142539.supplemental

#### References

**Amcheslavsky, A., Jiang, J. and Ip, Y. T.** (2009). Tissue damage-induced intestinal stem cell division in Drosophila. *Cell Stem Cell* **4**, 49-61.

**Antonello, Z. A., Reiff, T., Ballesta-Illan, E. and Dominguez, M.** (2015). Robust intestinal homeostasis relies on cellular plasticity in enteroblasts mediated by miR-8-Escargot switch. *EMBO J.* **34**, 2025-2041.

**Apidianakis, Y., Pitsouli, C., Perrimon, N. and Rahme, L.** (2009). Synergy between bacterial infection and genetic predisposition in intestinal dysplasia. *Proc. Natl. Acad. Sci. USA* **106**, 20883-20888.

**Bardin, A. J., Perdigoto, C. N., Southall, T. D., Brand, A. H. and Schweisguth, F.** (2010). Transcriptional control of stem cell maintenance in the Drosophila intestine. *Development* **137**, 705-714.

**Biteau, B., Hochmuth, C. E. and Jasper, H.** (2008). JNK activity in somatic stem cells causes loss of tissue homeostasis in the aging Drosophila gut. *Cell Stem Cell* **3**, 442-455.

**Boggiano, J. C. and Fehon, R. G.** (2012). Growth control by committee: intercellular junctions, cell polarity, and the cytoskeleton regulate Hippo signaling. *Dev. Cell* **22**, 695-702.

**Bonfini, A., Liu, X. and Buchon, N.** (2016). From pathogens to microbiota: how Drosophila intestinal stem cells react to gut microbes.*Dev. Comp. Immunol.* **64**, 22-38.

**Buchon, N., Broderick, N. A., Chakrabarti, S. and Lemaitre, B.** (2009a). Invasive and indigenous microbiota impact intestinal stem cell activity through multiple pathways in Drosophila. *Genes Dev.* **23**, 2333-2344.

**Buchon, N., Broderick, N. A., Poidevin, M., Pradervand, S. and Lemaitre, B.** (2009b). Drosophila intestinal response to bacterial infection: activation of host defense and stem cell proliferation. *Cell Host Microbe* **5**, 200-211.

**Buchon, N., Broderick, N. A., Kuraishi, T. and Lemaitre, B.** (2010). Drosophila EGFR pathway coordinates stem cell proliferation and gut remodeling following infection. *BMC Biol.* **8**,152.

**Buchon, N., Osman, D., David, F. P., Fang, H. Y., Boquete, J. P., Deplancke, P. and Lemaitre, B.** (2013). Morphological and molecular characterization of adult midgut compartmentalization in Drosophila. *Cell Rep.* **3**, 1725-1738.

**Bunker, B. D., Nellimoottil, T. T., Boileau, R. M., Classen, A. K. and Bilder, D.** (2015). The transcriptional response to tumorigenic polarity loss in Drosophila. *Elife* **4**.

**Celandroni, F., Salvetti, S., Senesi, S. and Ghelardi, E.** (2014). Bacillus thuringiensis membrane-damaging toxins acting on mammalian cells. *FEMS Microbiol. Lett.* **361**, 95-103.

**Chakrabarti, S., Liehl, P., Buchon, N. and Lemaitre, B.** (2012). Infection-induced host translational blockage inhibits immune responses and epithelial renewal in the Drosophila gut. *Cell Host Microbe* **12**, 60-70.

**Chatterjee, M. and Ip, Y. T.** (2009). Pathogenic stimulation of intestinal stem cell response in Drosophila. *J. Cell. Physiol.* **220**, 664-671.

**Collins, D., Hogan, A. M. and Winter, D. C.** (2011). Microbial and viral pathogens in colorectal cancer. *Lancet Oncol.* **12**, 504-512.

**Cordero, J. B., Stefanatos, R. K., Scopelliti, A., Vidal, M. and Sansom, O. J.** (2012). Inducible progenitor-derived Wingless regulates adult midgut regeneration in Drosophila. *EMBO J.* **31**, 3901-3917.
**Cronin, S. J. F., Nehme, N. T., Limmer, S., Liegeois, S., Pospisilik, J. A., Schramek, D., Leibbrandt, A., Simoes, R. M., Gruber, S., Puc, U. et al.** (2009). Genome-wide RNAi screen identifies genes involved in intestinal pathogenic bacterial infection. *Science* **325**, 340-343.
**Dutta, D., Dobson, A. J., Houtz, P. L., Gläßer, C., Revah, J., Korzelius, J., Patel, P. H., Edgar, B. A. and Buchon, N.** (2015). Regional cell-specific transcriptome mapping reveals regulatory complexity in the adult Drosophila midgut. *Cell Rep.* **12**, 346-358.
**Erkosar, B., Storelli, G., Mitchell, M., Bozonnet, L., Bozonnet, N. and Leulier, F.** (2015). Pathogen virulence impedes mutualist-mediated enhancement of host juvenile growth via inhibition of protein digestion. *Cell Host Microbe* **18**, 445-455.
**Frederiksen, K., Rosenquist, H., Jorgensen, K. and Wilcks, A.** (2006). Occurrence of natural Bacillus thuringiensis contaminants and residues of Bacillus thuringiensis-based insecticides on fresh fruits and vegetables. *Appl. Environ. Microbiol.* **72**, 3435-3440.
**Gaspar, P. and Tapon, N.** (2014). Sensing the local environment: actin architecture and Hippo signalling. *Curr. Opin. Cell Biol.* **31**, 74-83.
**Gonzalez, J. M., Jr., Brown, B. J. and Carlton, B. C.** (1982). Transfer of Bacillus thuringiensis plasmids coding for delta-endotoxin among strains of B. thuringiensis and B. cereus. *Proc. Natl. Acad. Sci. USA* **79**, 6951-6955.
**Igaki, T.** (2009). Correcting developmental errors by apoptosis: lessons from Drosophila JNK signaling. *Apoptosis* **14**, 1021-1028.
**Jiang, H., Patel, P. H., Kohlmaier, A., Grenley, M. O., McEwen, D. G. and Edgar, B. A.** (2009). Cytokine/Jak/Stat signaling mediates regeneration and homeostasis in the Drosophila midgut. *Cell* **137**, 1343-1355.
**Jiang, H., Grenley, M. O., Bravo, M.-J., Blumhagen, R. Z. and Edgar, B. A.** (2011). EGFR/Ras/MAPK signaling mediates adult midgut epithelial homeostasis and regeneration in Drosophila. *Cell Stem Cell* **8**, 84-95.
**Kango-Singh, M. and Singh, A.** (2009). Regulation of organ size: insights from the Drosophila Hippo signaling pathway. *Dev. Dyn.* **238**, 1627-1637.
**Karpac, J., Biteau, B. and Jasper, H.** (2013). Misregulation of an adaptive metabolic response contributes to the age-related disruption of lipid homeostasis in Drosophila. *Cell Rep* **4**, 1250-1261.
**Karpowicz, P., Perez, J. and Perrimon, N.** (2010). The Hippo tumor suppressor pathway regulates intestinal stem cell regeneration. *Development* **137**, 4135-4145.
**Kim, S. H. and Lee, W. J.** (2014). Role of DUOX in gut inflammation: lessons from Drosophila model of gut-microbiota interactions. *Front Cell Infect Microbiol.***3**, 116.
**Kux, K. and Pitsouli, C.** (2014). Tissue communication in regenerative inflammatory signaling: lessons from the fly gut. *Front Cell Infect Microbiol.* **4**, 49.
**Lee, K.-A., Kim, S.-H., Kim, E.-K., Ha, E.-M., You, H., Kim, B., Kim, M.-J., Kwon, Y., Ryu, J.-H. and Lee, W.-J.** (2013). Bacterial-derived uracil as a modulator of mucosal immunity and gut-microbe homeostasis in Drosophila. *Cell* **153**, 797-811.
**Lemaitre, B.** (2013). Morphological and molecular characterization of adult midgut compartmentalization in Drosophila. *Cell Rep.* **3**, 1725-1238.
**Marianes, A. and Spradling, A. C.** (2013). Physiological and stem cell compartmentalization within the Drosophila midgut. *Elife* **2**, e00886.
**McGuire, S. E., Le, P. T., Osborn, A. J., Matsumoto, K. and Davis, R. L.** (2003). Spatiotemporal rescue of memory dysfunction in Drosophila. *Science* **302**, 1765-1768.
**Micchelli, C. A.** (2014). Whole-mount immunostaining of the adult Drosophila gastrointestinal tract. *Methods* **68**, 273-279.
**Micchelli, C. A. and Perrimon, N.** (2006). Evidence that stem cells reside in the adult Drosophila midgut epithelium. *Nature* **439**, 475-479.
**Myant, K. B., Scopelliti, A., Haque, S., Vidal, M., Sansom, O. J. and Cordero, J. B.** (2013). Rac1 drives intestinal stem cell proliferation and regeneration. *Cell* **12**, 2973-2977.
**O'Brien, L. E., Soliman, S. S., Li, X. and Bilder, D.** (2011). Altered modes of stem cell division drive adaptive intestinal growth. *Cell* **147**, 603-614.
**Osman, D., Buchon, N., Chakrabarti, S., Huang, Y.-T., Su, W.-C., Poidevin, M., Tsai, Y.-C. and Lemaitre, B.** (2012). Autocrine and paracrine unpaired signaling regulate intestinal stem cell maintenance and division. *J. Cell Sci.* **125**, 5944-5949.
**Ota, M. and Sasaki, H.** (2008). Mammalian Tead proteins regulate cell proliferation and contact inhibition as transcriptional mediators of Hippo signaling. *Development* **135**, 4059-4069.
**Pasco, M. Y., Loudhaief, R. and Gallet, A.** (2015). The cellular homeostasis of the gut: what the Drosophila model points out. *Histol. Histopathol.* **30**, 277-292.
**Patel, P. H., Dutta, D. and Edgar, B. A.** (2015). Niche appropriation by Drosophila intestinal stem cell tumours. *Nat. Cell Biol.* **17**, 1182-1192.
**Raymond, B., Johnston, P. R., Nielsen-LeRoux, C., Lereclus, D. and Crickmore, N.** (2010). Bacillus thuringiensis: an impotent pathogen? *Trends* **18**, 189-194.
**Ren, F., Wang, B., Yue, T., Yun, E.-Y., Ip, Y. T. and Jiang, J.** (2010). Hippo signaling regulates Drosophila intestine stem cell proliferation through multiple pathways. *Proc. Natl. Acad. Sci. USA* **107**, 21064-21069.
**Ren, F., Shi, Q., Chen, Y., Jiang, A., Ip, Y. T., Jiang, H. and Jiang, J.** (2013). Drosophila Myc integrates multiple signaling pathways to regulate intestinal stem cell proliferation during midgut regeneration. *Cell Res.* **23**, 1133-1146.
**Shaw, R. L., Kohlmaier, A., Polesello, C., Veelken, C., Edgar, B. A. and Tapon, N.** (2010). The Hippo pathway regulates intestinal stem cell proliferation during Drosophila adult midgut regeneration. *Development* **137**, 4147-4158.
**Staley, B. K. and Irvine, K. D.** (2010). Warts and Yorkie mediate intestinal regeneration by influencing stem cell proliferation. *Curr. Biol.* **20**, 1580-1587.
**Stephan, D., Scholz-Döbelin, H., Kessler, H. and Reintges, T.** (2014). Investigations on residues of Bacillus thuringiensis on tomato. *DGaaE-Nachrichten* **28**, 56-56.
**Storelli, G., Defaye, A., Erkosar, B., Hols, P., Royet, J. and Leulier, F.** (2011). Lactobacillus plantarum promotes Drosophila systemic growth by modulating hormonal signals through TOR-dependent nutrient sensing. *Cell Metab.* **14**, 403-414.
**Sun, G. and Irvine, K. D.** (2014). Control of growth during regeneration. *Curr. Top. Dev. Biol.* **108**, 95-120. .
**Taylor, R. C., Cullen, S. P. and Martin, S. J.** (2008). Apoptosis: controlled demolition at the cellular level. *Nat. Rev. Mol. Cell Biol.* **9**, 231-241.
**Tjalsma, H., Boleij, A., Marchesi, J. R. and Dutilh, B. E.** (2012). A bacterial driver-passenger model for colorectal cancer: beyond the usual suspects. *Nat. Rev. Microbiol.* **10**, 575-582.
**Varelas, X., Samavarchi-Tehrani, P., Narimatsu, M., Weiss, A., Cockburn, K., Larsen, B. G., Rossant, J. and Wrana, J. L.** (2010). The Crumbs complex couples cell density sensing to Hippo-dependent control of the TGF-beta-SMAD pathway. *Dev. Cell* **19**, 831-844.
**Vriz, S., Reiter, S. and Galliot, B.** (2014). Cell death: a program to regenerate. *Curr. Top. Dev. Biol.* **108**, 121-151.
**Yu, F.-X. and Guan, K.-L.** (2013). The Hippo pathway: regulators and regulations. *Genes Dev.* **27**, 355-371.
**Zhao, B., Wei, X., Li, W., Udan, R. S., Yang, Q., Kim, J., Xie, J., Ikenoue, T., Yu, J., Li, L. et al.** (2007). Inactivation of YAP oncoprotein by the Hippo pathway is involved in cell contact inhibition and tissue growth control. *Genes Dev.* **21**, 2747-2761.
**Zhou, F., Rasmussen, A., Lee, S. and Agaisse, H.** (2013). The UPD3 cytokine couples environmental challenge and intestinal stem cell division through modulation of JAK/STAT signaling in the stem cell microenvironment. *Dev. Biol.* **373**, 383-393.

# EXPERIMENTAL PROCEDURES

## Fly stocks

- *Canton$^{S}$*
- *w; myo1A-Gal4 UAS-GFP/CyO (Y. Apidianakis)*
- *y w; esg-Gal4$^{NP5130}$ UAS-GFP/CyO (N. Tapon)*
- *y w; esg-lacZ$^{606}$/CyO (Y. Apidianankis)*
- *w; dl-Gal4/TM6b Tb (S. Hou et X. Zeng)*
- *w; myo1A-Gal4; tubGal80$^{ts}$ UAS-GFP/TM6b (N. Tapon)*
- *w; esg-Gal4 UAS-GFP; tubGal80$^{ts}$ (C. Michelli and Y. Apidianakis)*
- *w; act<STOP<lacZ; UAS-flp#5/(TM6b) (C. Micchelli)*
- *y w UAS-flp;; act5c<CD2<lacZ/TM6b (Y. Apidianakis)*
- *w;; puc-LacZ/TM3Sb (J. Colombani)*
- *dlg::GFP cc01936 (FlyTrap) (A. Spradling)*
- *w;; Diap1-lacZ/TM6B (J. Colombani)*
- *w; ex-lacZ/Cyo (N. Tapon & J. Colombani)*
- *w; ; UAS-Grim (T. Ip)*
- *w; ; UAS-p35 (T. Ip)*
- *w; ; UAS-dome$^{\Delta CYT\ 3\text{-}2}$/TM3 Sb (C. Ghiglione)*
- *yw hs-flp; UAS-hpo$^{RNAi}$ (VDRC 104169, KK)*
- *yv;; UAS-sav$^{RNAi}$ (Bloomington 32965)*
- *y v;; UAS-yki$^{RNAi}$ (y$^{+}$)/TM3 Sb TRIP (Bloomington 36965)*
- *hs-flp122; UAS-yki::HA/SM6-TM6 (N. Tapon)*
- *w; UAS-puc$^{2A}$ (R. Rousset)*
- *w, UAS-Diap1$^{myc}$ (T. Adachi-Yamada)*
- *y w hs-flp; tub-Gal80$^{ts}$/CyO; Dl-Gal4 UAS-GFP/TM6c (home made)*
- *w; act<CD2<Gal4; UAS-GFP (V. Van de Bor)*
- *yv/yw hs flp; UAS-hpo$^{RNAi}$/CyO; UAS-yki$^{RNAi}$/TM6B or C (home made)*
- *y w hep$^{1}$/FM7$^{wa}$ (R. Rousset)*
- *-yw; UAS-Ras$^{85D.V12}$ (Bloomington 4847)*
- *w; 10XStat-destabilizedGFP/Cyo (N. Tapon)*
- *w; upd1-Gal4 UAS-GFP (D. Osman)*

More information on Drosophila genes and stocks are available on FlyBase (http://flybase.org/).

**Genotypes of used F1 flies:**

- Fig. 2B and Fig. S2C and D: *w/w; esg-Gal4 UAS-GFP/+; tubGal80$^{t}$/UAS-dome$^{\Delta CYT\ 3\text{-}2}$*
- Fig. 2E-H" and Fig. S2 F-H' Fig.: *w/w; myo1A-Gal4 UAS-GFP/esg-lacZ$^{606}$*
- Fig. 3E (column *myo1A$^{ts}$>GFP>grim*) and Fig. S4C and D: *w/w; myo1A-Gal4/+; tub Gal80$^{ts}$ UAS-GFP/UAS-Grim*
- Fig. 3F-L and Fig. S4F-H'.: *w UAS-flp/w; esg-Gal4 UAS-GFP/+; tub-Gal80$^{ts}$/act5c<CD2<lacZ* or *w/w; esg-Gal4 UAS-GFP/act5c<CD2<lacZ; tub-Gal80$^{ts}$/UAS-flp*
- Fig. 4J-L and Fig. S5A and B: *w/w; myo1A-Gal4/+; tub-Gal80$^{ts}$ UAS-GFP/UAS-p35*
- Fig. 4M and N: *w/w; esg-Gal4 UAS-GFP/+; tubGal80$^{t}$/UAS-dome$^{\Delta CYT\ 3\text{-}2}$*
- Fig. 4O and P: *w/w; tub-Gal80$^{ts}$/UAS-Ras$^{85D.V12}$; dl-Gal4 UAS-GFP/+*
- Fig. 4Q-Q": *w/w; myo1A-Gal4 UAS-GFP/esg-lacZ$^{606}$*
- Fig. 4R and R": *w UAS-flp/w; esg-Gal4 UAS-GFP/+; tub-Gal80$^{ts}$/act5c<CD2<lacZ* or *w/w; esg-Gal4 UAS-GFP/act5c<CD2<lacZ; tub-Gal80$^{ts}$/UAS-flp*
- Fig. 5C: *w/w; myo1A-Gal4/UAS-puc$^{2A}$; tub-Gal80$^{ts}$ UAS-GFP/+*
- Fig. 5D- E": *w/w; myo1A-Gal4 UAS-GFP/+; Diap1-lacZ/+*
- Fig. S6 D-E": *w/w; myo1A-Gal4 UAS-GFP/ex-lacZ*
- Fig. 5F: *w UAS-Diap1$^{myc}$ /w; myo1A-Gal4/+; tub-Gal80$^{ts}$ UAS-GFP/+*
- Fig. 5G and H: *w/w ; myo1A-Gal4/UAS-yki::HA; tub-Gal80$^{ts}$ UAS GFP/+*
- Fig. 5I and J: *w/w; myo1A-Gal4/+; tub-Gal80$^{ts}$ UAS-GFP/UAS-yki$^{RNAi}$*
- Fig. 5K-N and Fig. S6F: *w/w; myo1A-Gal4/UAS-hpo$^{RNAi}$; tub-Gal80$^{ts}$ UAS-GFP/+*
- Fig. S6G-G": *y w hs-flp/w; act<CD2<Gal4/UAS-hpo$^{RNAi}$; UAS-GFP/+*
- Fig. S6H and I: *w/w; myo1A-Gal4/+; tub-Gal80$^{ts}$ UAS-GFP/UAS-sav$^{RNAi}$*
- Fig. S6J and K: *w/w; myo1A-Gal4/ UAS-hpo$^{RNAi}$; tub-Gal80$^{ts}$ UAS GFP/UAS-yki$^{RNAi}$*

**Table S1. RT-qPCR Primers**

| | | |
|---|---|---|
| *dp1* | Forward | ACG-GGC-AGA-ATT-GAG-AAG-TG |
| | Reverse | GGT-ACG-ATG-GAG-GTC-GAA-AG |
| *rp49* | Forward | CGC-ACC-AAG-CAC-TTC-ATC |
| | Reverse | CAC-TCT-GTT-GTC-GAT-ACC-CTT-G |
| *puc* | Forward | GCCACATCAGAACATCAAGC |
| | Reverse | CCGTTTTCCGTGCATCTT |
| *upd1* | Forward | CCT-ACT-CGT-CCT-GCT-CCT-TG |
| | Reverse | GCC-GTA-CTG-GAG-GTG-GTG |
| *upd3* | Forward | ACC-ACC-AAT-GCG-GAC-AAG |
| | Reverse | ATT-CAG-ACG-GGG-CAG-GAA |
| *Diap1* | Forward | GAA-CGC-GAC-CCA-GCT-ATT-C |
| | Reverse | CGT-TTA-TCC-AGC-CAG-TCC-A |
| *expanded* | Forward | TGG-TCT-TCC-TTG-CTG-GAC-TT |
| | Reverse | AGA-TGC-CGA-TGT-CTC-CTC-TC |
| *trypsine ε* | Forward | CGT-ATC-GTC-GGT-GGT-TAT-GAG |
| | Reverse | CAA-TGT-CGT-GGG-AGT-AGA-TGG |
| *lipase A* | Forward | CAG-ATA-CAC-TAC-GCC-GGA-CA |
| | Reverse | TCG-AAG-AAG-GCA-CAT-GGA-G |

# SUPPLEMENTAL FIGURES

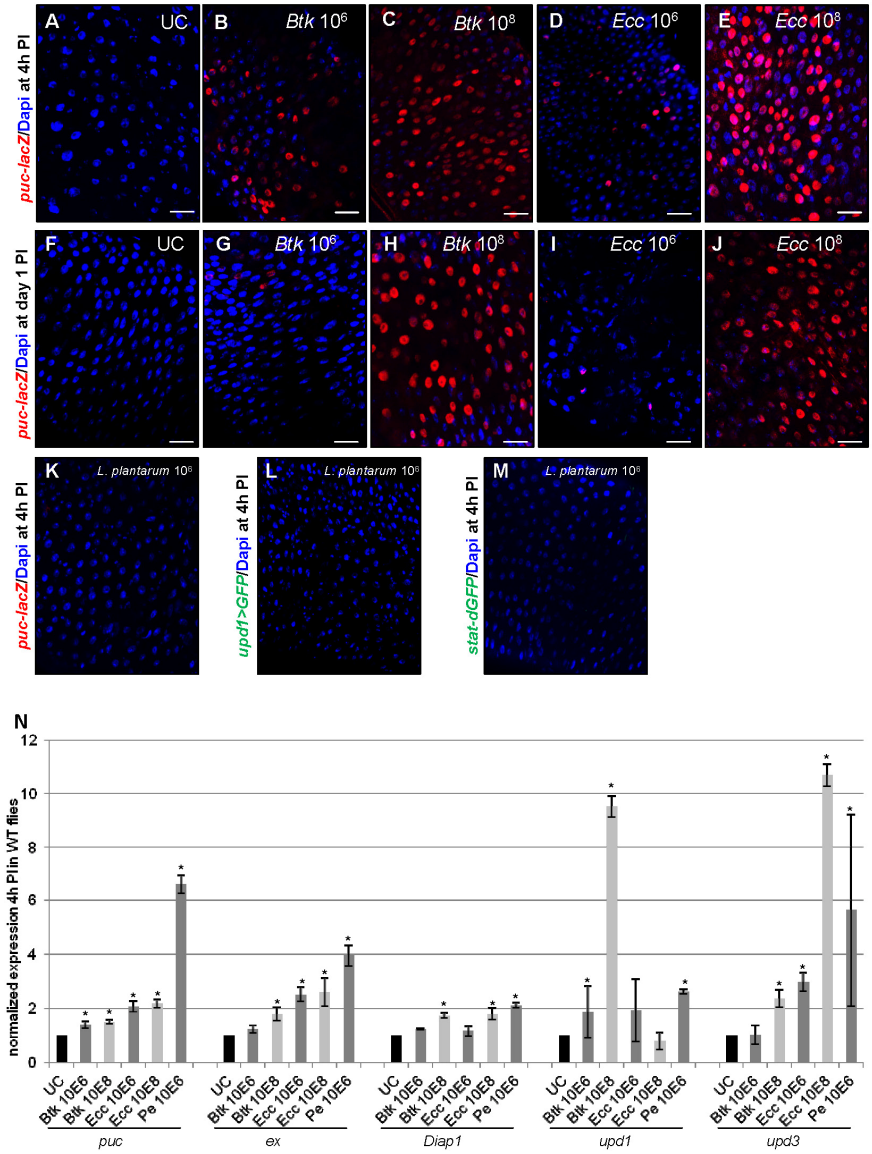


**Fig. S1: Low amounts of opportunistic bacteria induces a mild early stress response in the Drosophila posterior midgut**

**(A-J)** *puc-lacZ* posterior midguts stained for β-Gal (red) and DNA (blue) 4h PI of sucrose (A), *Btk* $10^6$ CFU (B), *Btk* $10^8$ CFU (C), *Ecc*$10^6$ CFU (D) and *Ecc* $10^8$ CFU (E), or 1 day PI of sucrose (F), *Btk* $10^6$ CFU (G), *Btk* $10^8$ CFU (H), *Ecc*$10^6$ CFU (I) and *Ecc* $10^8$ CFU (J). Scale bar =25µm. (**K-M**) *puc-lacZ* (labeled for β-Gal in red) (K), *upd1>GFP* (L) and *dSTAT-GFP* (M) posterior midguts from flies fed with *L. plantarum* $10^6$ CFU 4h PI. DNA labeling in blue (Dapi). Note that there is no activation of stress signaling pathways. (**N**) RT-qPCR on posterior midguts 4h PI of WT flies fed with sucrose (UC), Btk $10^6$ CFU, *Btk* $10^8$ CFU, Ecc$10^6$ CFU, Ecc$10^8$ CFU and Pe $10^6$ CFU showing normalized expression of *puc*, *ex*, *Diap1*, *upd1* and *upd3* (n=30).

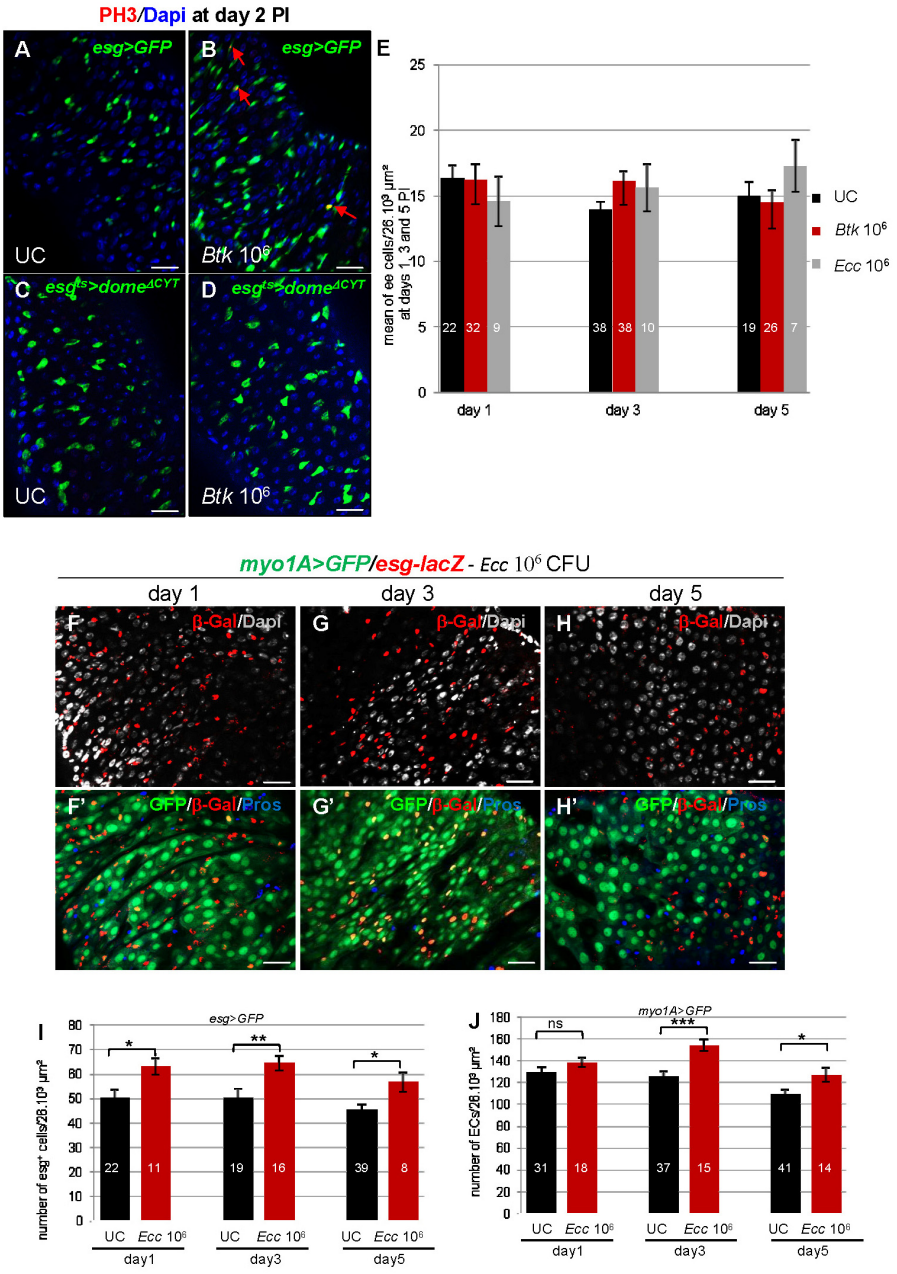


**Fig. S2: Mild-stress induces ISC proliferation and an accumulation of enterocytes**

**(A-B)** *esg>GFP* posterior midguts 2 days PI of sucrose (A) and *Btk* $10^6$CFU (B) labeled for the PH3 (red, arrows) and Dapi (blue). **(C-D)** *esg$^{ts}$>dome$^{\Delta CYT}$* posterior midguts 2 days PI of sucrose (C) and *Btk* $10^6$CFU (D) labeled for the PH3 (red) and DAPI (blue). **(E)** Quantification of entero-endocrine cells (Pros+) at day 1, day 3 and day 5 PI of *Btk* $10^6$ CFU. **(F-H')** *myo1A>GFP, esg-lacZ* posterior midguts stained for β-Gal (red), Pros (blue) and Dapi (white) at days 1, 3 and 5 PI of *Ecc* $10^6$ CFU. **(I)** Quantification of *esg+* cells in the posterior midguts of *esg>GFP* flies at days 1, 3 and 5 PI of sucrose (UC) or *Ecc* $10^6$CFU. **(J)** Quantification with ECs in the posterior midguts of *myo1A>GFP* flies at days 1, 3 and 5 PI of sucrose (UC) or *Ecc* $10^6$CFU. Scale bar =25µm.

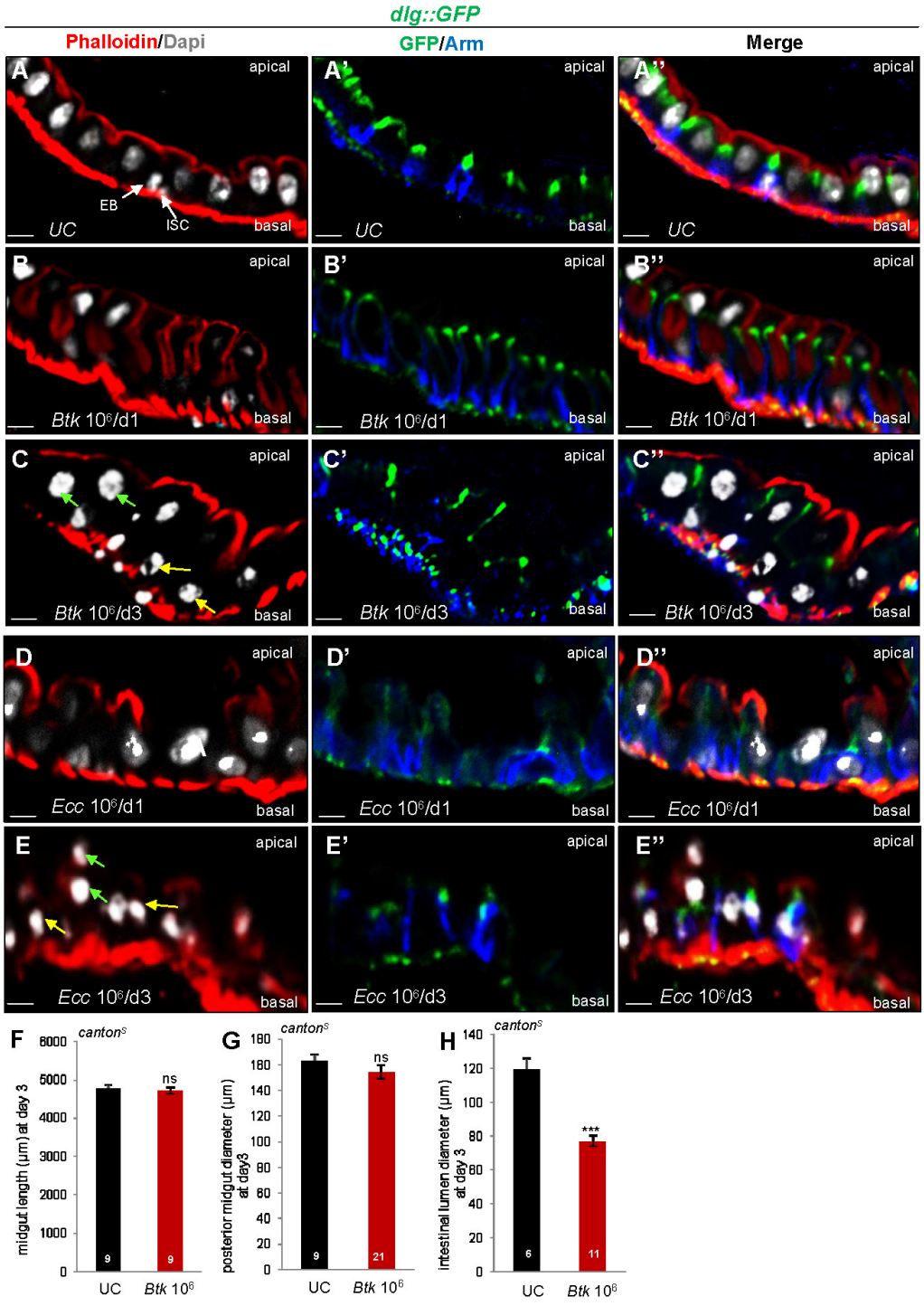


**Fig. S3: Structural consequences of EC accumulation**

(**A-E"**) Cryogenic cross-section of *dlg::GFP* posterior midguts. (A-A") UC, (B-C") *Btk* $10^6$ CFU fed flies 1day (B-B") and 3 days (C-C") PI. (D-E") *Ecc* $10^6$CFU fed flies 1day (D-D") and 3 days (E-E") PI. Guts are labeled with Phalloidin (red, apical pole and visceral mesoderm marker), Dapi (white), Arm (blue, basolateral marker) and Dlg::GFP (green, sub-apical marker). White arrows point the progenitor cells, yellow arrows point the eEC and green arrows point the old EC, scale bar=7,14µm. In control posterior midguts, the big polyploid EC nuclei were well aligned with the smaller diploid progenitor cell (ISC and EB)

nuclei located basally (A). At day 1 PI of *Btk* or *Ecc*, ECs became thinner, rounder, more elongated and with an extended apical pole (B-B" and D-D"). At day 3 PI the alignment of nuclei was perturbed (C-C" and E-E") and we often observed three rows of nuclei: an apical row of very large polyploid EC nuclei (green arrows in C and E), a second row of smaller polyploid nuclei corresponding to eECs (yellow arrows in C and E) and a third basal row of progenitor cells with small diploid nuclei. (**F-H**) Measurement of midgut length (F), posterior width (G) and posterior luminal diameter (H) of UC or *Btk* $10^6$ CFU fed flies. The length and the width are unaffected by the ingestion of Btk (F and G) while a significant reduction of the luminal diameter is observed upon the ingestion of *Btk* (H).

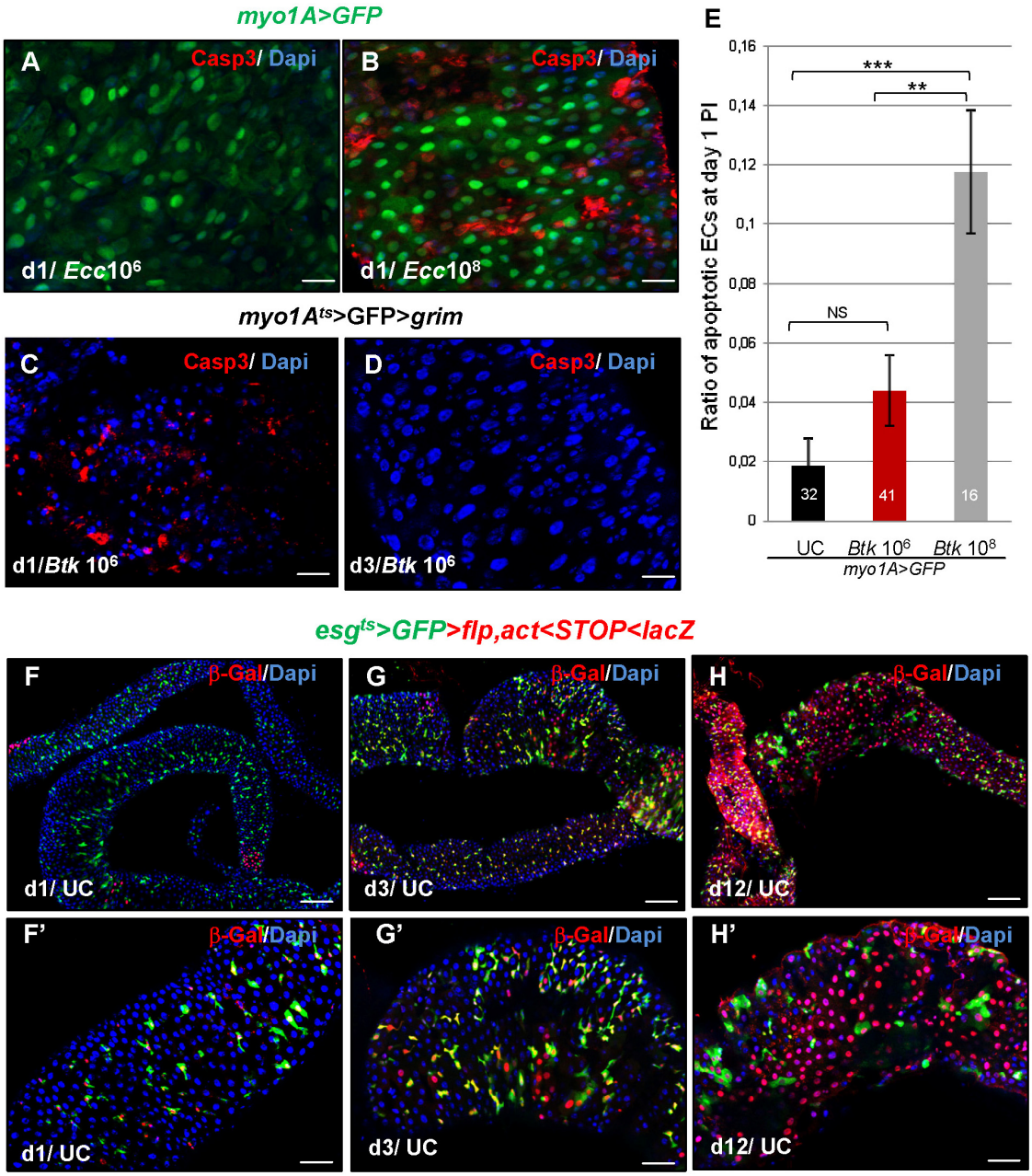


**Fig. S4: Early absence of cell death is responsible for EC accumulation**

**(A-B)** *myo1A>GFP* posterior midguts stained for Casp 3 (red) and Dapi (blue) at day 1 PI of *Ecc* $10^6$CFU (A) and *Ecc* $10^8$CFU (B). Scale bar =25µm. **(C-D)** *myo1A$^{ts}$>GFP>grim* posterior midguts stained for Casp 3 (red) and Dapi (blue) at day 1 and day 3 PI of *Btk* $10^6$CFU (see Figure 4D for the steps of the experiment), scale bar =25µm. **(E)** Ratio of apoptotic ECs at day 1 PI of *Btk* $10^6$CFU and *Btk* $10^8$CFU. **(F-H')** Cell lineage in *esg$^{ts}$>GFP>FLP, act<CD2<lacZ* guts of flies fed with sucrose (UC) at day 1 (F and F'), day 3 (G and G') and day 12 (H and H') at 29°C. Guts are stained for β-Gal (Red) and Dapi (Blue). Scale bar =100µm in F, G and H and =50µm in F', G' and H'.

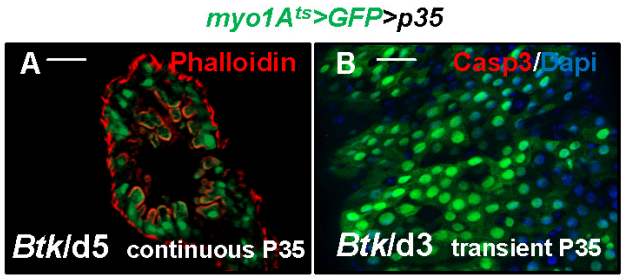


**Fig. S5: A late wave of cell death eliminates supernumerary ECs**

**(A)** Cryogenic cross-section of *myo1A*$^{ts}$*>GFP>p35* posterior midguts 5 days PI of *Btk* $10^6$CFU. Guts were labeled with Phalloidin (red). GFP marks the ECs. (**B**) *myo1A*$^{ts}$*>GFP>p35* posterior midguts stained for Casp3 (red) and Dapi (blue) at day 3 PI of *Btk* $10^6$CFU. Apoptosis were transiently inhibited by p35 according to the protocol described in the main figure 6B. Scale bar =30µm.

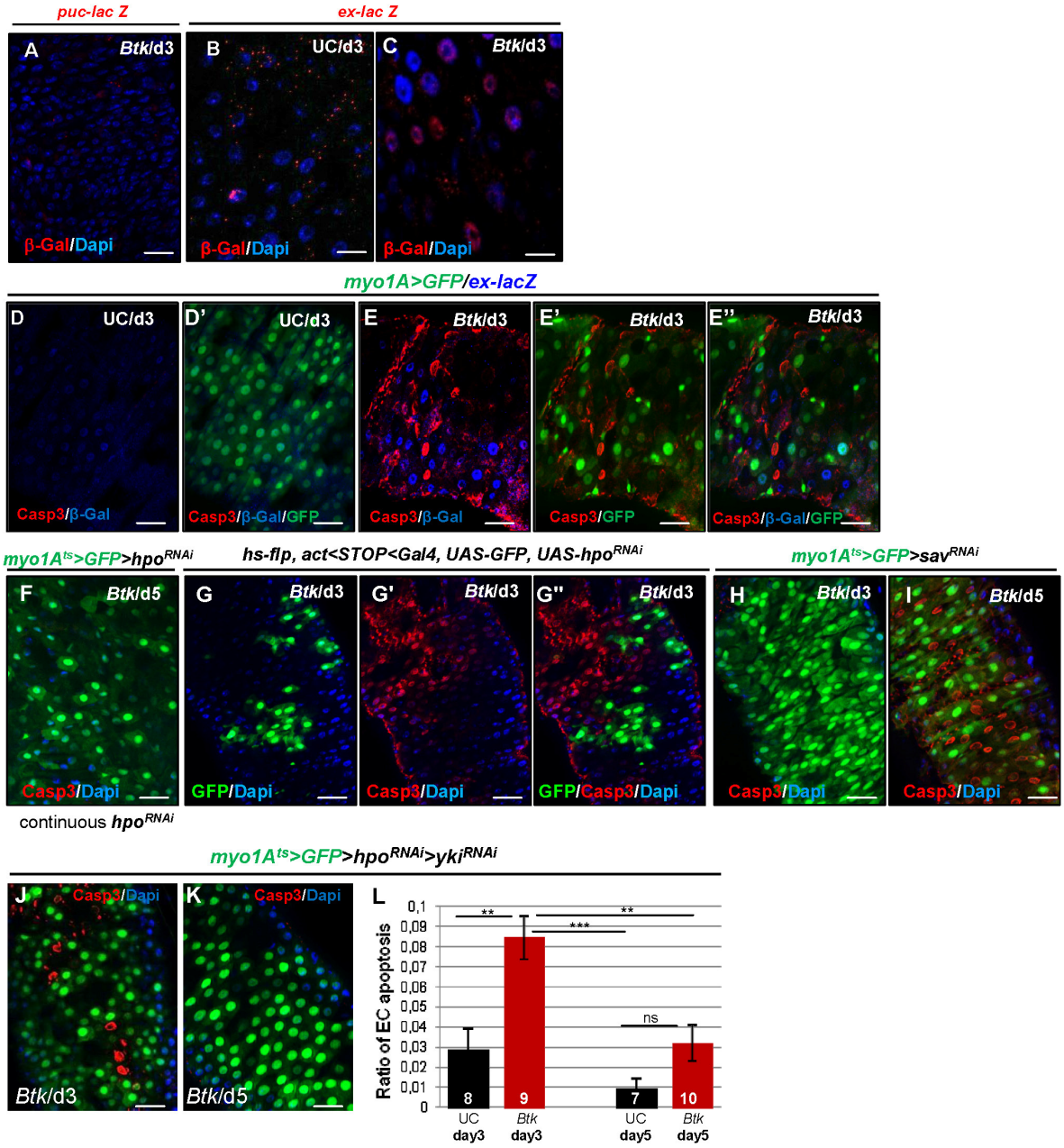


**Fig.S6: Hpo is involved in EC apoptosis in response to their excess**

(**A**) *puc-lacZ* posterior midguts stained for β-Gal (red) and Dapi (blue) 3 days PI of *Btk* $10^6$ CFU. Scale bar =30µm. (**B-C**) *ex-lacZ* posterior midguts of flies fed with sucrose (UC) or *Btk* $10^6$ CFU 3 days PI. Guts are labeled for β–Gal (pink) and Dapi (blue). **(D-E")** *myo1A>GFP; ex-lacZ* midguts stained for β-Gal (blue) and Casp3 (red) 3 days PI of sucrose (UC), *Btk* $10^6$ CFU. (**F**) *myo1A$^{ts}$>GFP>hpo$^{RNAi}$* posterior midguts. After continuous induction *hpo$^{RNAi}$*, posterior midguts were stained for Casp3 (red) and Dapi (blue) at day 5 PI of *Btk* $10^6$ CFU. (**G-G"**) *hs-flp, act<STOP<Gal4, UAS-GFP, UAS-hpo$^{RNAi}$* posterior midguts stained for Casp3 (red) and Dapi (blue) 3 days PI of *Btk* $10^6$ CFU. No overlaps between *hpo$^{RNAi}$* cells (GFP+) and Casp 3 staining (red) are observed. DNA is marked with Dapi (blue). (**H** and **I**)

*myo1A*$^{ts}$>*GFP*>*sav*$^{RNAi}$ posterior midguts at day 3 (H) and day 5 (I) PI of *Btk* $10^6$ CFU. Guts are labeled for Casp3 (red) and Dapi (blue). (**J and K**) *myo1A*$^{ts}$>*GFP* posterior midguts of flies overexpressing the double *hpo*$^{RNAi}$, *yki*$^{RNAi}$ and fed with $10^6$CFU of *Btk* 3 days PI (J) or 5 days PI (K). (**L**) Ratio of apoptosis in posterior midguts at days 3 and 5 PI in UC (left) and $10^6$CFU *Btk* (right) fed *myo1A*$^{ts}$>*GFP*>*hpo*$^{RNAi}$>*yki*$^{RNAi}$ flies.

(A-C) Scale bar=12,5µm. (D-K) scale bar=30µm.